



**REVIEW OF AERONAUTICAL FATIGUE INVESTIGATIONS
IN POLAND
DURING THE PERIOD MAY 2009 TO MARCH 2011**

by
Dr Antoni Niepokólczycki
Institute of Aviation, Warsaw, POLAND

For Presentation at the 32 Conference of
the International Committee on Aeronautical Fatigue
Montreal, Canada, 30-31 May 2011

Approved for Public Release

CONTENTS

1. INTRODUCTION.....	3
2. HELICOPTERS	4
2.1 Fatigue Life Estimation of the Tail Boom and Vertical Stabilizer of Mi-24 Helicopter	4
2.2 Fatigue Life Assessment of Selected Structural Elements of Mi-24 Helicopter.....	6
2.3 Experimental and Numerical Crack Initiation Analysis of the Compressor Blades Working in Resonance Conditions.....	7
2.4 Stress Intensity Factor Calculations for the Compressor Blade with Half-Elliptical Surface Crack using Raju-Newman Solution	10
3. AIRPLANE STRUCTURES.....	12
3.1 Estimation of Fatigue Properties of Composite Structures	12
3.2 Diagnosis and Repair Technology of Damaged Elements of CASA Aircraft	14
3.3 Crack Growth Analysis of the Landing Gear Pull Rod of the Fighter Jet Aircraft.....	15
3.4 Service Life Assessment Program of PZL-130 ORLIK TCII Structure	17
3.5 Representative Load Sequence for the PZL-130 ORLIK	18
3.6 Flight Loads Acquisition for PZL-130 ORLIK TC-II Full Scale Fatigue Test.....	19
3.7 PZL-130 ORLIK TCII Fracture Markers Solution for Full-Scale Fatigue Test	21
3.8 The Cracks Propagation Calculations in the PZL-130 ORLIK Structure	22
4. MATERIALS TESTING	24
4.1 Investigations of Some Properties of Material Samples Taken from the Aircraft Withdrawn from Service	24
4.2 Predicting Fatigue Crack Growth and Fatigue Life under Variable Amplitude Loading ..	26
4.3 The Analysis of a Fatigue Crack Propagation in the Elements of Aluminum Alloy D16CzATW with a Notch in the Form of a Cylindrical Hole	27
5. JOINTS.....	28
5.1 Investigation into Fatigue Behaviour of Metal-Composite Glue Connection.....	28
5.2 Experimental and Numerical Study of Stress and Strain Field around the Rivet	29
6. NON-DESTRUCTIVE TESTS AND STRUCTURAL HEALTH MONITORING	30
6.1 Diagnostics of Composite Aircraft Structures using Non-Destructive Tests with Thermographic, Ultrasound and Acoustic Methods	30
6.2 Analysis of the Possibility to Assess the Occurrence of Hidden Corrosion in Lap Joints using Active Thermography.....	32
6.3 Structural Health Monitoring Approach to the Aerospace Structures	33
7. THE SYNTHETIC DESCRIPTION OF THE RESULTS, SCIENTIFIC ACHIEVEMENTS AND PRACTICAL APPLICATIONS THE EUREKA INITIATIVE, THE PROJECT IMPERJA, E3496!, <i>IMPROVING THE FATIGUE PERFORMANCE OF RIVETED JOINTS IN AIRFRAMES</i>	38

1. INTRODUCTION

This review gives the summary of work performed in Poland in the area of aeronautical fatigue during the period from May 2009 to March 2011.

The various contributions to this review come from the following sources:

Air Force Institute of Technology, Warsaw;
Warsaw University of Technology, Warsaw;
Military University of Technology, Warsaw;
Rzeszow University of Technology, Rzeszow;
Institute of Aviation, Warsaw;

The names of the principal investigators and their affiliations are presented in brackets at the end of each chapter.

Full addresses of contributors are available through the author of this review at:

Antoni NIEPOKÓLCZYCKI
Institute of Aviation
Al. Krakowska 110/114
02-256 Warsaw, POLAND

Phone: (+48 22) 846 08 01 ext. 546

Mobile: +48 695 905 440

Fax: (+48 22) 846 75 36

E-mail: antekn@ilot.edu.pl

2. HELICOPTERS

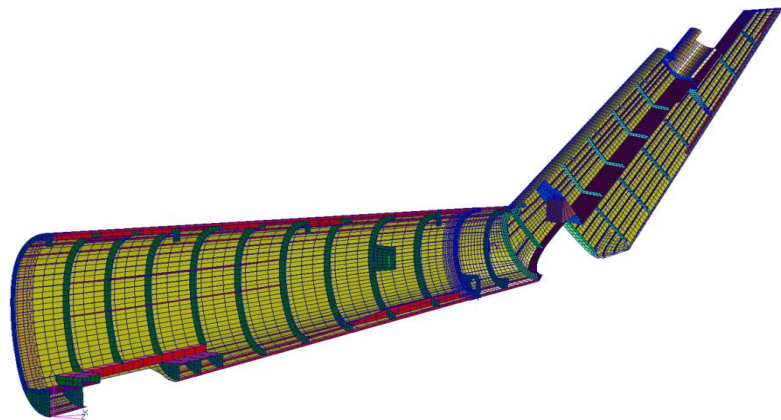
2.1 Fatigue Life Estimation of the Tail Boom and Vertical Stabilizer of Mi-24 Helicopter



Mi-24 helicopters have been exploited all around the world for decades. Data that come from the manufacturer are strictly dependent on the assumed flight profile so the estimated fatigue life may vary from the expected one. It is known that for two different load spectra, fatigue life of a specimen will differ so in order to estimate a reliable fatigue life one must take into consideration specific conditions in which the specimen, in this case a helicopter, will operate.

The aim of this work was to estimate fatigue life of the Mi-24 helicopter tail boom and vertical stabilizer sheathing. The analysis was based on a numerical model of the helicopter airframe used to obtain stress fields under defined loads and to estimate fatigue life. The numerical model, stress estimations and fatigue calculations were made with the MSC software. Altogether, the model of the tail boom and vertical stabilizer consisted of about 24 000 elements.

View of the right hand side half of the numerical model

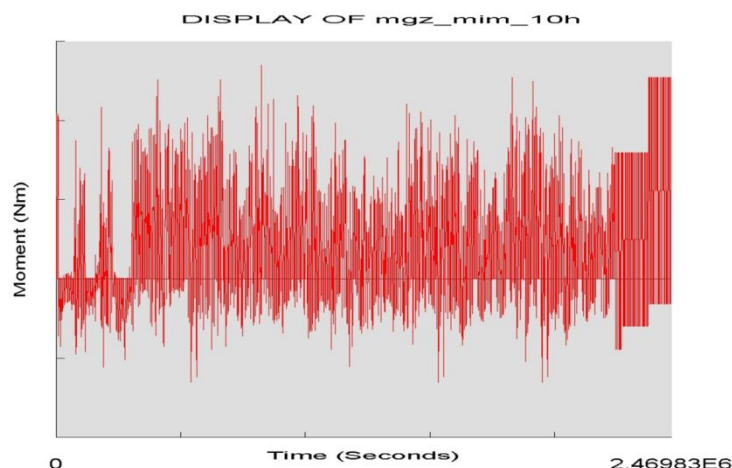


The majority of the elements used in the model were thin walled quad elements with six degrees of freedom in a node in order to consider the effect of bending. The strength elements such as ribs or transmission boxes were represented by brick elements. Bar and beam elements were introduced for slender structure elements, such as stringers reinforcements, or when the geometry of an element was not relevant but its mass was significant, like in the case of the horizontal stabilizer.

The Air Force Institute of Technology decided to evaluate a representative ten-hour spectrum characteristic for the Mi-24 helicopters. In order to do so, an array of strain gauges was designed and installed onto the airframe to gather coherent strain signals during flight.

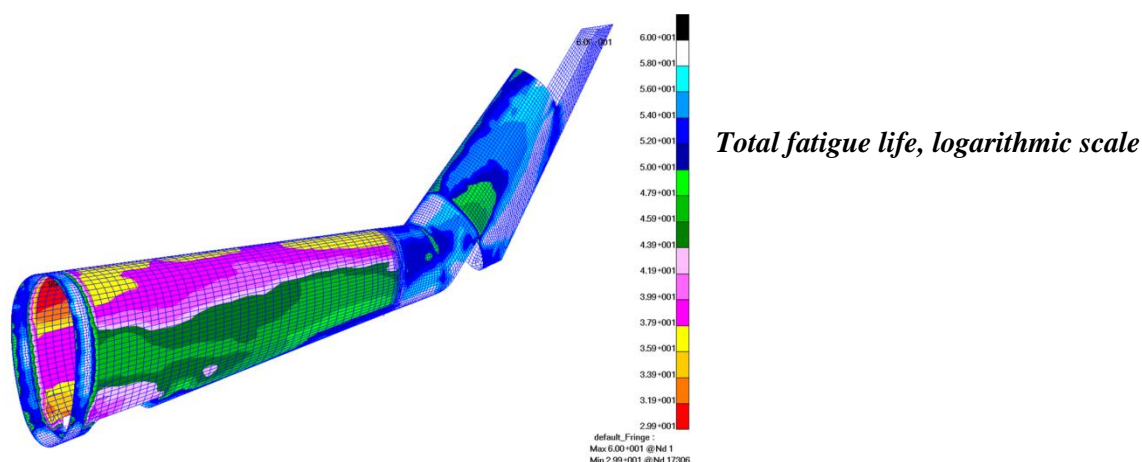
After installation, the system was scaled using defined loads applied to the structure, which enabled creating linear regression equations describing flight loads by means of measured strains. The experimental flights were specially designed to fully represent the missions and particular maneuvers that are most common during exploitation. After the flights, data was gathered and post-processed and three ten-hour load spectra were obtained, representing statistical loading of the airframe.

Example load spectrum for the bending moment in horizontal plane



The last crucial element of the analysis, the S-N curve, was determined using the MSC/Fatigue software.

As a result of the calculations, the fatigue life for each load was obtained.



The analysis determined the critical locations where fatigue damage may occur. Damaged regions were located in the vertical stabilizer, where the horizontal part meets the skew one and on the circumference of the tail boom near the collar connecting it to the rest of the fuselage.

The presented estimation allowed predicting fatigue life of the sheathing to be 6200 flight hours. The load that had most influence on the airframe fatigue life was the bending moment in the horizontal plane caused by the rear rotor thrust.

(Research supervised by Andrzej Leski, Air Force Institute of Technology, Warsaw).

2.2 Fatigue Life Assessment of Selected Structural Elements of Mi-24 Helicopter

The aim of this work was to assess fatigue life of selected structural elements of the Mi-24 helicopter based on the real load spectra.

The actual levels of loads acting on the elements during the flight were measured. The entire test was performed using the numerical analysis. Fatigue life was determined using the MSC/FATIGUE program with the Palmgren - Miner linear damage accumulation rule.



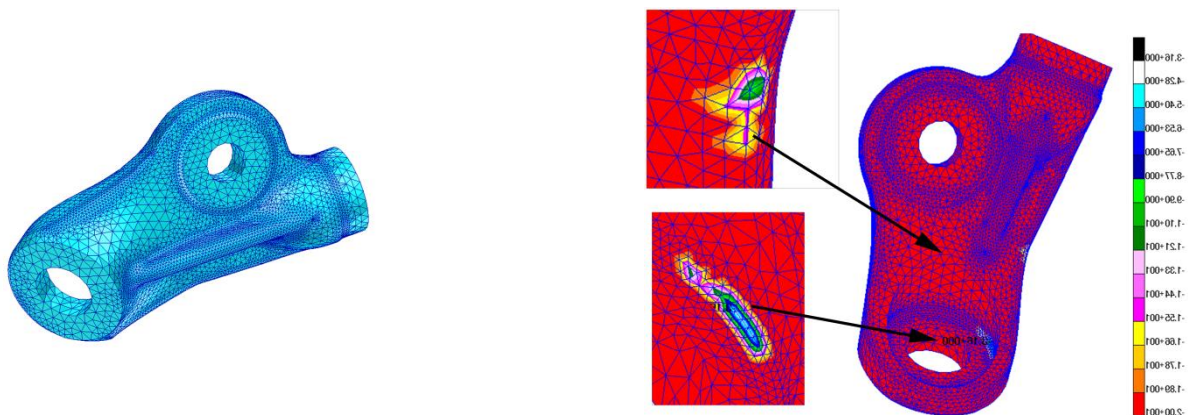
The selected structural elements are:

- Lever arm of the swash plate collective pitch control of the helicopter rotor.
- Secondary strut of the main gear support frame.
- Primary strut of the main gear support frame.
- Pull rod for longitudinal control.
- Pull rod for lateral control.
- Pull rod for directional control.



The actual load spectra were developed based on flight test results. All selected elements were taken off the helicopter. The strain gauges were glued onto the chosen surfaces. Then a calibrating procedure was carried out using laboratory facilities. During this procedure loads were applied by the MTS testing machine and signals from the strain gauges were recorded. As a result of the calibrating procedure, the regression equations were developed. Using these equations, the forces acting on the elements during flight could be calculated based on the recorded strain gauges signals.

The measurements of loads in the selected structural elements were conducted during the flight tests performed by the Air Force Institute of Technology in 2009.



The fatigue damage calculations were performed using the MSC/Fatigue software.

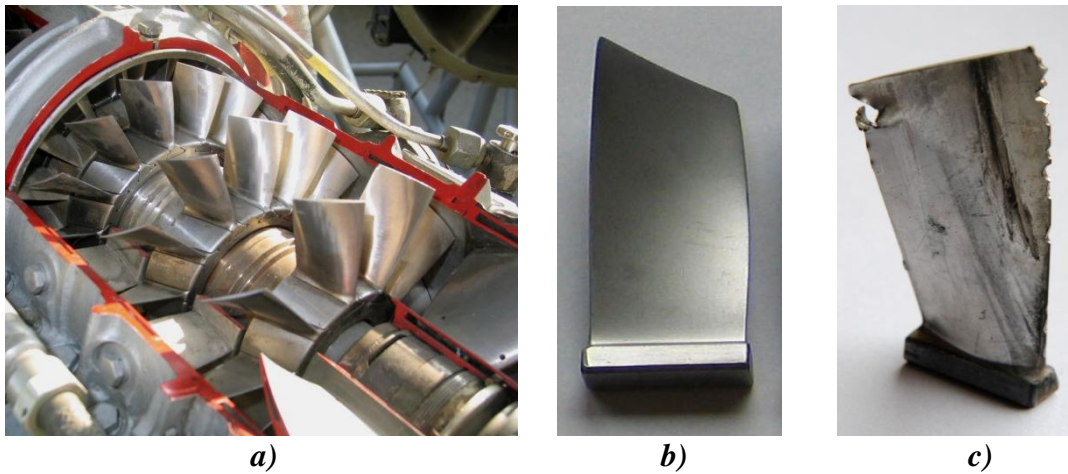
The results of the numerical calculations showed that some elements had unlimited fatigue life but there were also some elements where the significant fatigue damage could be a problem. The calculated fatigue life is highly dependent on assumptions made while developing the safe S-N curve. In this analysis, high safety factors result in short fatigue life estimations for some elements.

The additional value of the work on stress analyses was developing by the Air Force Institute of Technology the NDT programme for the Mi-24 helicopter. Based on the stress analysis results, the NDT activity can be focused on the areas where the high stress levels occur.

(Research supervised by Andrzej Leski, Air Force Institute of Technology, Warsaw).

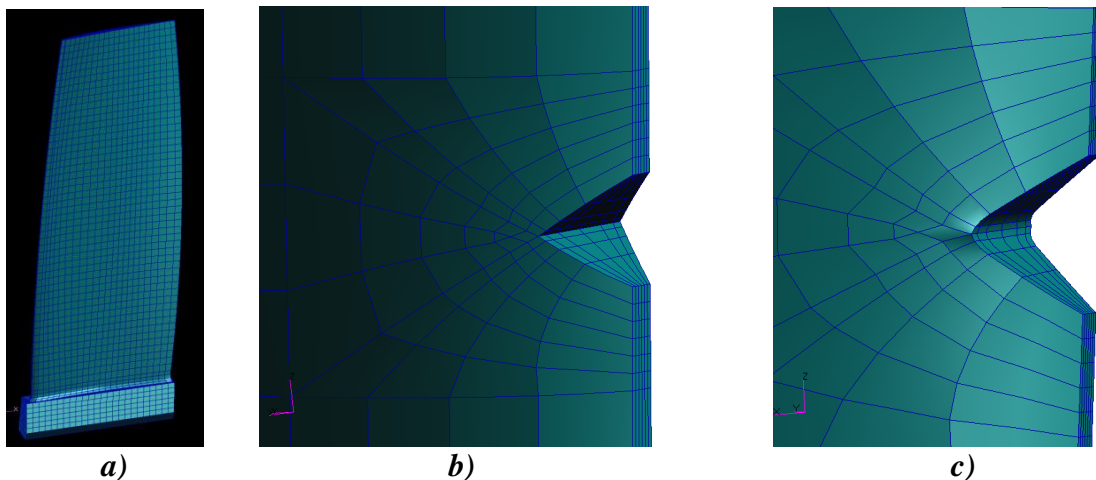
2.3 Experimental and Numerical Crack Initiation Analysis of the Compressor Blades Working in Resonance Conditions

This work focused on a complex experimental and numerical crack initiation analysis of the helicopter turbo-engine compressor blades subjected to vibrations.



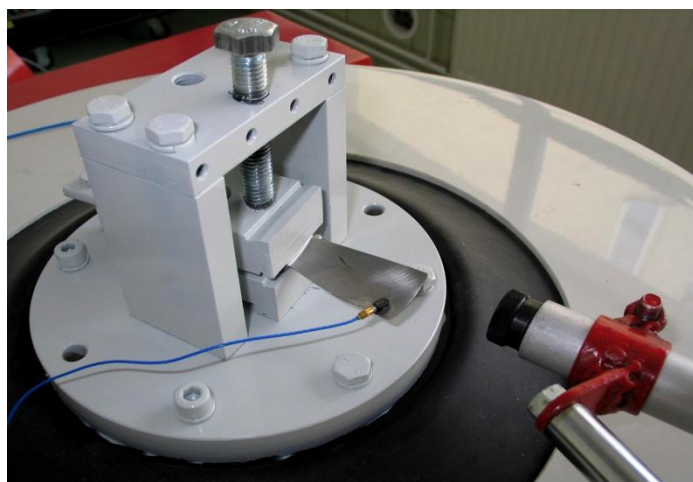
View of the first stages of aeroengine axial compressor (a), separated blade without mechanical defects (b) and the blade damaged by a foreign object (c).

A nonlinear finite element method was utilized to determine the stress state of the blade during the first mode of transverse vibration. In this analysis, the numerical models without defects as well as those with V-notches were defined.



Numerical model of the non-defected blade (a) and magnified view of model with infinite (b) and finite notch radius (c).

The quality of the numerical solution was checked by the convergence analysis. The obtained results were subsequently used as input data into crack initiation (ϵ -N) analyses performed for the load time history equivalent to one cycle of the transverse vibration. In the fatigue analysis, the Neuber elastic-plastic strain correction method, linear damage summation and Palmgreen-Miner rule were utilized. As a result of ϵ -N analysis, the number of load cycles to the first fatigue crack appearing in the compressor blades was obtained. Moreover, the influence of the blade vibration amplitude on the number of cycles to the crack initiation was analyzed. Values of the fatigue properties of the blade material were calculated using the Baumele-Seeger and Muralidharan methods. The influence of both the notch radius and values of the UTS of the blade material on the fatigue behavior of the structure was also considered. In the last part of the work, the finite element results were compared with the results of the experimental vibration HCF tests performed for the compressor blades.



Compressor blade fixed to the shaker during the fatigue test

Based on the analysis performed, the following conclusions have been formulated:

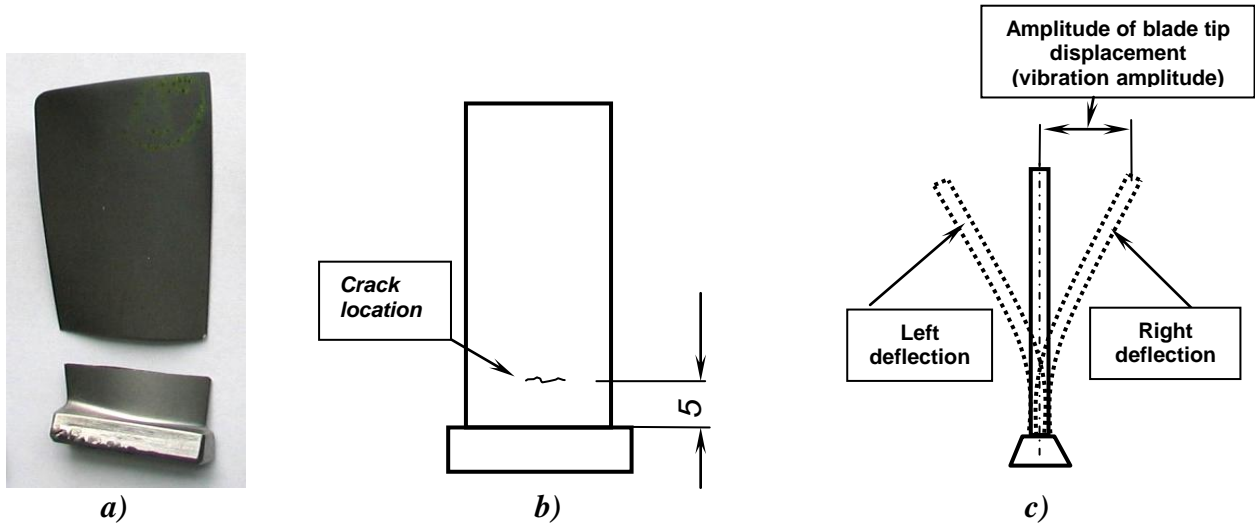
1. The quality of the FE model was checked by convergence analysis. In this analysis, the resonant frequency (f_{rez}) obtained from numerical calculations was compared with the value of f_{rez} received during the experimental investigations. The result of this analysis showed that, in the range of 2000-12000 finite elements, the value of f_{rez} quickly decreased. In the presented case, satisfactory results can be obtained when the model has more elements than 13000.
2. The maximum tensile stress in the blade vibrated with an amplitude of 1 mm is about 248 MPa. When the blade has a notch with the radius of 0 mm, the computed stress near the notch tip is about 3 times larger (878 MPa). The most unfavorable case is when the blade is damaged by a sharp foreign object during the engine operation and the notch has a radius close to zero.
3. The maximum principal stress area in the non-defected blade (248 MPa, the connection between the blade profile and the dovetail) is not the same as the zone where the cracks were appearing during the fatigue experimental tests (the zone located between 1 mm and 15 mm above the dovetail, in the central part of the convex blade surface). This difference might be due to inaccurate radius modeling in the zone of the profile-dovetail connection.
4. The estimated number of cycles to the crack initiation for the blade without the mechanical defects is about 1,4 million (mln), (for the blade vibrated with an amplitude of 2 mm). The results of ϵ -N analysis strongly depend on the amplitude of the blade tip displacement. For larger amplitudes, the difference between the actual stress in the blade and the UTS of the blade material decreases. When the amplitude increases to the value of 4 mm, the fatigue durability of the blade decreases to about 4700 cycles.

5. The estimated fatigue life of the blade with a notch or FOD is very low. For the notched blade vibrated with an amplitude of 1mm (for notch radius $r=0\text{mm}$), the estimated number of cycles to the crack initiation is 12882. It means that the blade vibrated with resonant frequency equal to about 800 Hz, will work for only 12 seconds to the first crack appearance. When the notch radius is 0,075 mm, the crack will initiate after about 49000 cycles.
6. The results of ε -N analysis strongly depend on the Ultimate Tensile Strength (UTS, R_m) of the blade material. The estimated number of cycles to the crack initiation (for the following parameters: UTS = 1090 MPa, vibration amplitude of 2 mm, the Baumeel-Seeger approximation, not defected blade) is about 1,4 mln. cycles. When the UTS decreases to 1000 MPa, the initiation process begins at 0,6 mln cycles. The result of ε -N analysis for UTS=950 MPa is about 0,4 mln of cycles. The actual UTS of the EI-961 alloy depends on its heat treatment. The quality of the heat treatment should be controlled during manufacturing process because of its significant influence on the fatigue life.
7. The observed variation in the experimental results exceeds 300%. In the experimental fatigue analysis, this dispersion is typical. Thus, it is difficult to compare the experimental and numerical results due to a small number of experimental tests (only 10 investigated blades without preliminary defects and 10 with notches).
8. Based on the obtained results, it seems that the numerical fatigue calculations are conservative. The results of calculations for the non-defected blade (using the Baumeel-Seegel method) are about 100% lower than the number of cycles to the crack initiation obtained in the experiment. The Muralidharan method gives more significant errors (200%) than the Baumeel-Seegel properties estimation.
9. The results divergence might be due to inaccurate fatigue material properties estimation. The experimental tests (or a different analytical method to obtain these properties) should be performed before next analysis.
10. The blade was shot-peened during manufacturing process. Shot peening introduces the compressive (residual) stress into the surface layer of the material. Superposition of the actual (tensioned) stress and the residual (compressed) stress causes that the fatigue life of the shot-peened components is longer. In the ε -N analysis, the effect of the residual stresses was not considered. This fact might account for the divergence between the numerical and experimental results.
11. The divergence between numerical and experimental fatigue results for the blades with notches is very big (300-500%). One of possible reasons for the low fatigue resistance estimation is that during the notch creation process (the notch was created when a sharp object hit the attached edge of the blade) a very large plastic strain is observed. In consequence, a large zone of compressive (residual) stresses is formed in the notch vicinity. The effect of the residual stresses on the fatigue life of the blade should be also investigated.

(Research supervised by Lucjan Witek, Rzeszow University of Technology, Rzeszów).

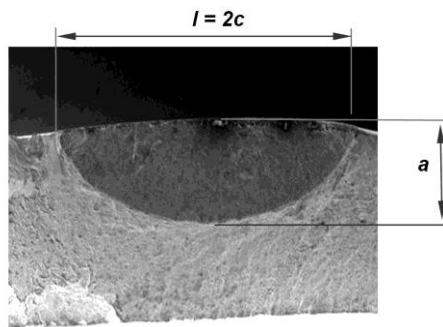
2.4 Stress Intensity Factor Calculations for the Compressor Blade with Half-Elliptical Surface Crack using Raju-Newman Solution

In this study, the stress intensity factor for the 1st stage compressor blade was computed. In this analysis, the Raju-Newman analytical solution was used. A half-elliptical surface crack was embedded in the analyzed blade.



First stage compressor blade after fatigue test (a), the most frequent crack location in the blade without preliminary defects (b) and the 1st mode of transverse vibrations shape (c).

The location of this crack and the crack front shape were defined based on the experimental results obtained for the blade tested in resonance conditions. The K-factor values were computed only at one point of the crack front, where the crack tip touches the free surface as the crack length was measured just in this direction ($\phi = 0$) during experimental investigations. In order to determine the stress intensity factors for different crack sizes, ten diverse flaws in the blade were defined.



A half-elliptical crack emanating from the convex blade surface, in the preliminary phase of fracture.

In the next part of this work, the stress intensity factor values were used as input data into the Paris-Erdogan equation. As a result of this calculation, the crack growth rate for the compressor blade vibrating at constant amplitude was estimated. The obtained results were finally compared with the results of the

experimental crack growth analysis performed for 1st stage compressor blades of the helicopter turbo-engine.

The analytical estimation using the Raju-Newman and Paris equations gives the fatigue cycle values which are about 30% lower than those obtained in the experimental tests. This divergence could be caused by inaccurate definitions of C and m constants in the Paris equation. Moreover, the replacement of the actual blade cross-section with the rectangular shape affects the accuracy of the analytical solution. After the omission of the first increment (concerning crack growth from initiation to length $l=1,3$ mm), the difference between the analytical and numerical solution is much smaller.

The author's intention is to calculate (in the next study) the stress intensity factor in the compressor blade using the hybrid method. In this approach, the finite element method will be

used for stress analysis. Subsequently, the boundary element method will be utilized for the crack definition and also for the stress intensity factor calculation. The obtained numerical results can be compared with the K-factor values computed from the Raju-Newman solution. *(Research supervised by Lucjan Witek, Rzeszow University of Technology, Rzeszów).*

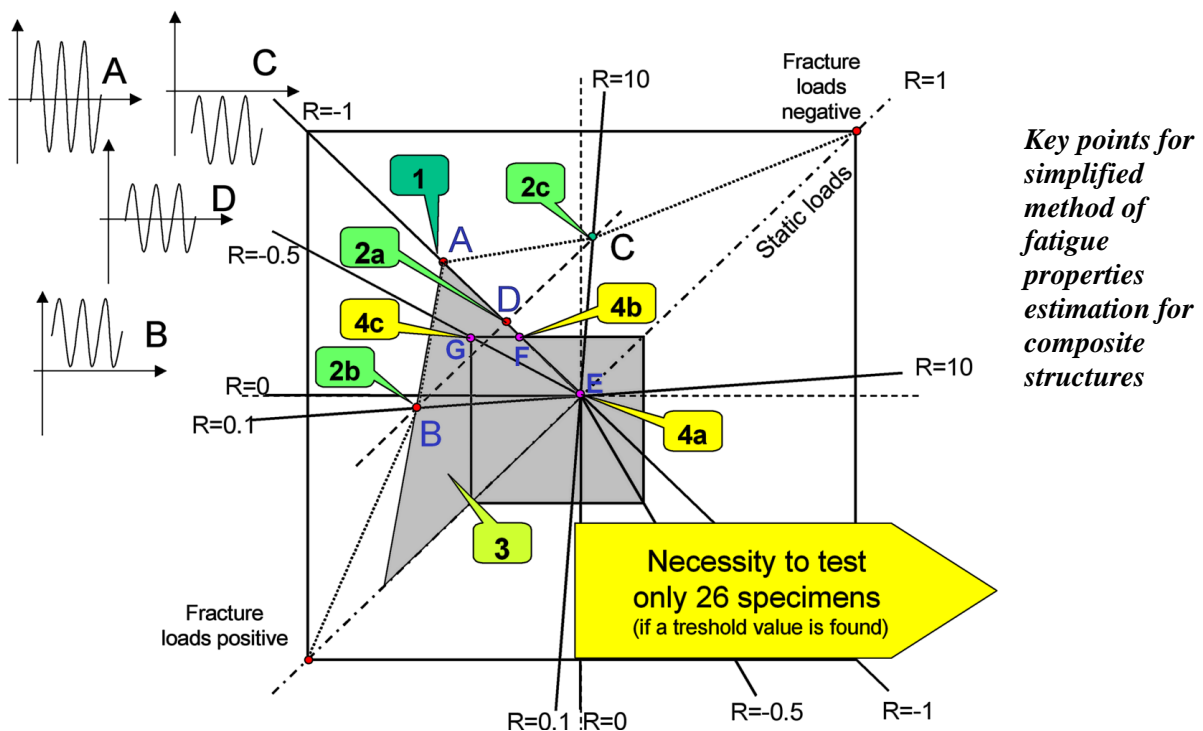
3. AIRPLANE STRUCTURES

3.1 Estimation of Fatigue Properties of Composite Structures

The work focused on a simplified method of fatigue properties estimation for polymer composite structures.

The simplified methodology of the fatigue properties estimation relies on the estimation of the virtual surface, which describes in an approximate way the number of cycles to failure in the operational zone of loads in the High diagram. This estimation is based on the results of fatigue tests.

The 1st step of the simplified procedure of the fatigue properties investigation consists in the determination of the threshold value of the material fatigue sensitivity for $R = -1$. It is represented by point A in the figure below, and it could be interpreted as the loads that cause a noticeable drop in the residual strength after 10^4 cycles.

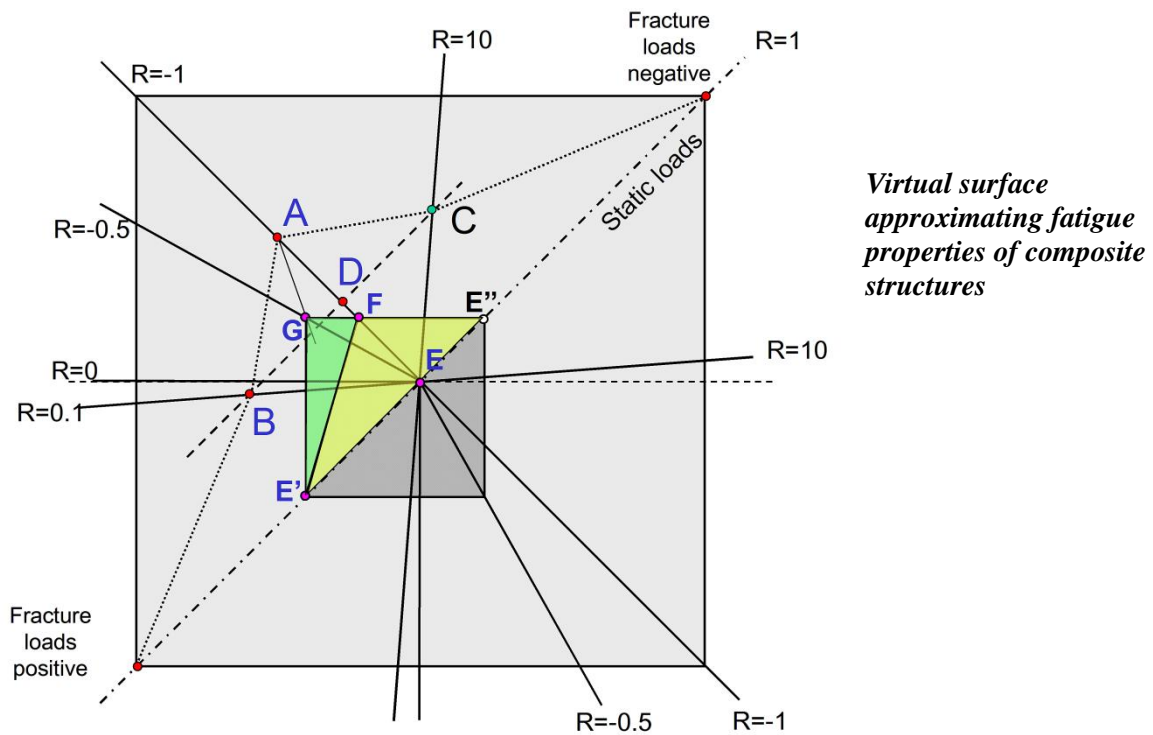


The 2nd step consists in the determination of loads which exert the same influence on the residual strength after 10^4 cycles at point A as at point B, which lies on the line representing $R = 0.1$ (and as at point C if necessary), and then as at point D. It is worth emphasising that points B, C, D are situated along a line of constant load amplitude, which facilitates the fatigue testing.

The 3rd step consists in spreading the virtual plane based on points A, B, D. It is assumed that the vertical coordinate represents the logarithms of cycles to failure.

The 4th step of this procedure consists in the determination of the number of cycles to failure at points E, F, and G, which belongs to the plane ABD.

In the last (i.e. 5th) step of the procedure, two virtual planes $E'GF$ and $E'FE''$ are created, which make up the surface representing the number of cycles to failure in the zone of operational loads (see figure below).



It was assumed that the number of cycles to failure is constant along the 0-diagonal and is the same as at point E.

We can conclude that the simplified methodology of the fatigue properties estimation for polymer composite structures, although not perfect, seems to be reasonable. Future experimental investigations will verify the expectations related to the described method.
(Research supervised by Mirosław Rodzewicz, Warsaw University of Technology, Warsaw).

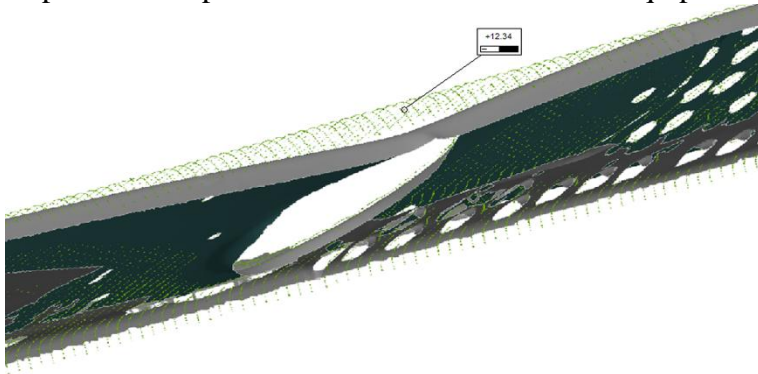
3.2 Diagnosis and Repair Technology of Damaged Elements of CASA Aircraft



The C-295 aircraft used by the Polish Air Forces caught fire. During take-off, the breaks broke down and got blocked, which caused burning of the composite panels. Although the fire was not big, the composite panels and the metal longeron as well as the elements inside the left gear's deflector required nondestructive inspection and repair.

The investigated panel is a CFRP sandwich structure. Tests for disbonds between the core and the skin were made. The elementary visual inspection provided information about a large area of disbond. Next step was a quantification with the Bond Master equipment, and the manual Tap Testing (for the confirmation of the results).

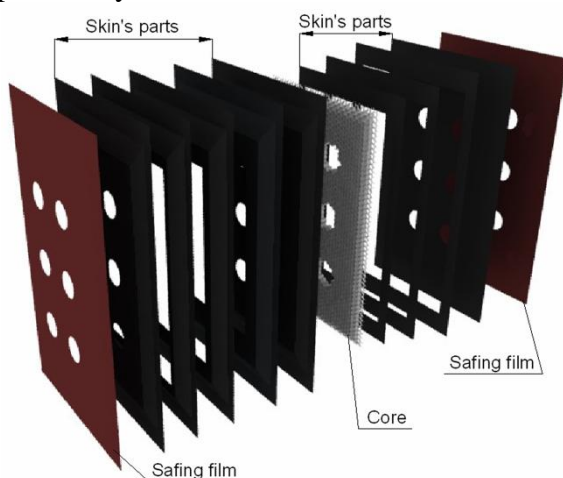
The second object under investigation was the longeron. For the longeron, the conductivity inspection was performed with the Phasec 2200 equipment.



Deformation of the longeron caused by the heat treatment

Based on performances obtained from NDT, the technology of repairing the longeron and composite elements was developed.

Although the fire caused failure in three composite elements, this work focused on the vertical panel only.



Panel's structure

The failure found could be repaired by different methods: replacing the damaged part with a new one, filling up with resin gaps between the skin and the core or removing and reconstructing the damaged panel's parts: the skin, core and protective layer.

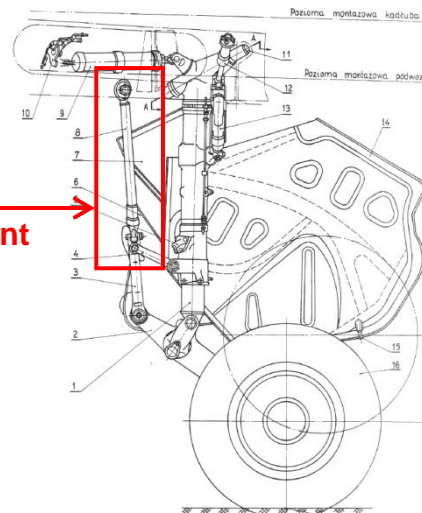
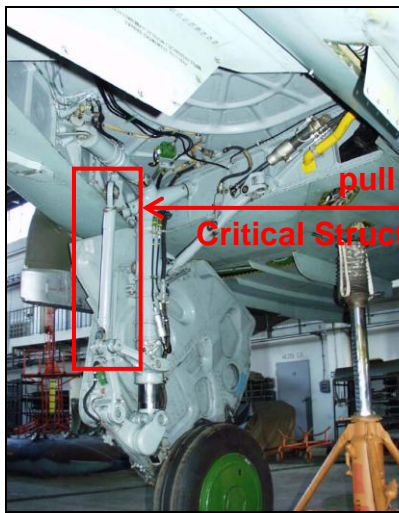
The latter is the best method.

The properties of the patch are always different from the original structure, so the panel must be monitored after repair.

(Research supervised by Michał Salaciński, Air Force Institute of Technology, Warsaw).

3.3 Crack Growth Analysis of the Landing Gear Pull Rod of the Fighter Jet Aircraft

Sukhoi Su-22 FITTER is a single engined supersonic fighter-bomber jet airplane. The aircraft was manufactured in the former Soviet Union in several variants. It has been operated by the former Warsaw Pact countries as well as by some countries in the Middle East and Africa.

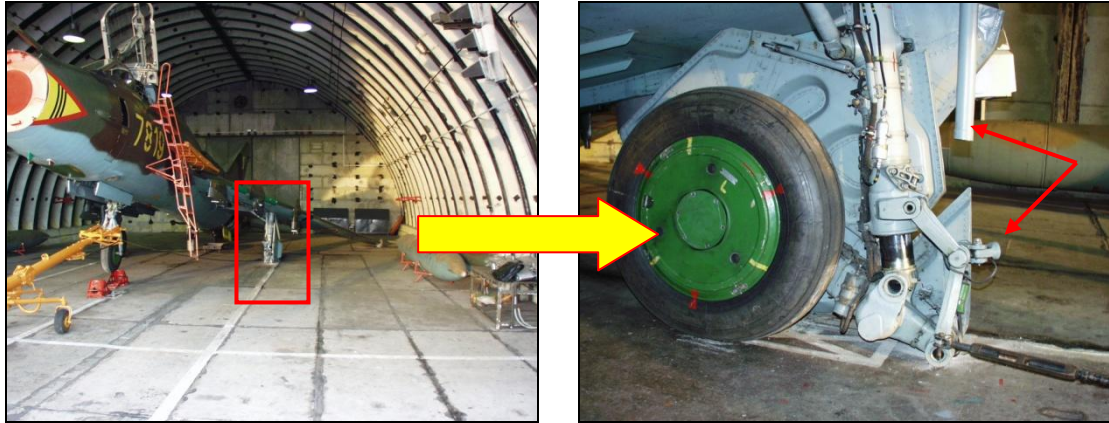


Main landing gear scheme

The pull rod is the member responsible for transmitting the load to the wing's strength members. It consists of two structural elements, the lower eye and the pull rod cylinder (tube). These two elements are joined by welding. The tube is fastened to the other (upper) eye with a threaded connection, which permits regulation of the pull rod's length.

The problem investigated is related to two incidents, the first of which (in 2004) was a surprise for the operator. During a morning inspection of the hangar buildings, it was observed that the aircraft was lying in an untypical position. Preliminary visual inspection revealed a rupture of the pull rod of the left main landing gear. After the inspection, the aircraft was elevated and restored to its proper position and the damaged component was replaced.

It is important to note that the described incident took place when the aircraft was on standby in the hangar, a few days after the aircraft's last flight. This indicates that the critical crack length had almost been reached, yet without the crack being noticed. Prior to the emergence of the critical crack on the pull rod, the aircraft had been in service for 19 years during which time there were about 1700 take-offs and landings. The in-flight time for the described aircraft amounted to almost 1300 hours, with the designed service life being 2000 hours.



Failure of the main landing gear

The problem re-emerged in 2010. As was the case in the earlier incident, a rupture of the pull-rod of an in-service aircraft occurred. As before, a few days after the last flight a disjuncting of the pull rod elements took place. This time, the incident happened on an aircraft that had been in service for 34 years/~1300 flight hours. In this service period the aircraft performed 1716 landings.

The material tests and other engineering analyses pointed to the fatigue fracture as the cause of damage. The cracking process originated in the area of a structural notch on the boundary of the pull-rod base material and one of the three spot welds. The calculated crack propagation time (number of cycles) for the case was determined to be considerable. The corrosion of the inner surface of the cylinder was the factor that accelerated the crack growth. The occurrence of yet another rupture showed that the problem is more severe than initially assumed. The crack growth calculations suggest that there exists a factor that accelerates the crack growth. Stress-corrosion appears to be the factor in question. The investigation of the first (2004) incident did not determine the presence of stress corrosion. Corrosion was detected in the second (2010) case only. Contribution of stress-corrosion to the crack growth process is very likely as significant tensile stresses occur in the pull rod discussed during the aircraft hangar standby. The Su-22 aircraft are stored in non-conditioned hangar-shelters. The presence of stress-corrosion influences the determination of the NDI inspection interval. The exact determination of the corrosion's influence on the rate of crack propagation in the pull rod requires additional research.

(Research supervised by Marcin Kurdelski, Air Force Institute of Technology, Warsaw).

3.4 Service Life Assessment Program of PZL-130 ORLIK TCII Structure

The work concerns the structural integrity program (SEWST) for the PZL-130 ORLIK TCII trainer aircraft.

The PZL-130 ORLIK was designed by PZL Warszawa-Okecie as a trainer aircraft for the Polish Air Force. In 1994 it was introduced to service in the Polish Air Force (version TCI). It is a single-engine, two-seater aircraft for initial pilot training.

Experience gained over 15 years of operation has demonstrated that its maintenance and overhaul system might be improved.

An upgraded version of TCI is the TCII version. Major differences as compared to TCI are:

- changes in the wing shape and rudder leading to improvement in maneuverability
- change of the engine and the propeller (PT6-25C Pratt & Whitney, Hartzell)
- brand new wings
- new digital avionics (GPS/VOR/ILS).

Alongside the modernization of the aircraft, the Polish Air Force decided to develop a new maintenance system for PZL-130 ORLIK. The main requirements of the new system are:

- Developing and applying Aircraft Structural Integrity Program – ASIP) according to MIL- STD -1530C.
- Cancellation of overhauls.
- Confirmation of total service life of the structure during Full Scale Fatigue Test – minimum 6000fth (with safety factor).

The realization of these objectives is the subject of the research program SEWST (abbreviation denoting the Polish language system for operating the aircraft based on their actual health). The SEWST program has been carried out by EADS PZL “Okecie” and the Air Force Institute of Technology.

The whole SEWST program covers many different areas. Its most important part is the Service Life Assessment program. Its key components are:

- Preparation of load spectrum
- Full Scale Fatigue Tests
- Teardown Inspections
- Numerical analyses
- Corrosion Prevention & Control Program (CPCP)
- Non Destructive Inspections (NDI) and System for Health Monitoring (SHM)

The contractor for FSFT is VZLU Praha (Czech Republic). During the test the structure will be periodically checked by the NDT personnel. The inspection plan is prepared by the AFIT. The inspections will be performed by both the VZLU and AFIT technicians.

After the FSFT has been completed the structure will be checked during the Teardown Inspection. TI is a destructive examination of the structure. The structure will be cut into small parts suitable for inspections in the lab facility.



The SEWST program started at the end of 2009. The instrumentation of the aircraft was carried through in the spring 2010. Simultaneously, the flight test program was developed. The calibration and flight test were completed in the early autumn 2010. The test article was produced by EADS PZL-Okęcie and delivered to VZLU at the end of 2010. The FSFT starts in the spring 2011.

(Research supervised by Andrzej Leski, Air Force Institute of Technology, Warsaw).

3.5 Representative Load Sequence for the PZL-130 ORLIK



The aim of developing the representative load sequence (RLS) for the PZL-130 ORLIK was to obtain a load time history which would be the best approximation of loads acting on the aircraft structure during average flight. This load time history should be short enough to be used for numerical calculation or laboratory tests. Good approximation can be achieved if a large number of performed flights were taken into consideration.

Such a large number of recorded flights can be collected during long operational usage. Otherwise good approximation can be assessed based on an extensive flight test program. Developing RLS consists in extracting crucial (for fatigue and crack growth analyses) information from the collected data. The information which must be retained in RSL is:

- a number of fatigue cycles of a particular amplitude and mean value,
- a cycle sequence.

The developed data base of PZL-130 ORLIK consists of more than 35000 collected downloads (each download comprises one flight). Because PZL-130 ORLIK is a trainer, all performed flights were training missions. All collected downloads contain information about the exercises performed by the pilot. This way, statistics for exercise frequency can be calculated.

At the beginning of developing the representative load sequence for PZL-130 ORLIK the following assumptions were made:

- a) Flight loads can be characterized by Nz-cycle;
- b) RLS should consist of 100-150 flight sequence;
- c) Flights selected for RLS should match the statistics for exercise frequency;
- d) Nz-cycle statistics for RLS should match the nz-cycle statistics for all collected flights.

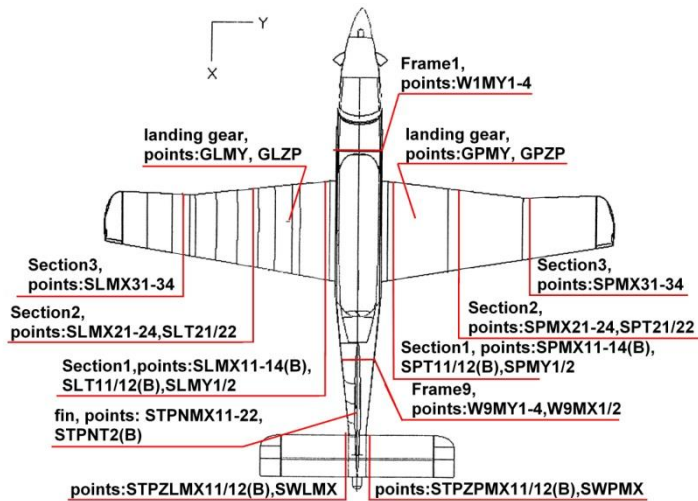
The real RLS was obtained for the trainer PZL-130 ORLIK using an algorithm. 3353 recorded real flights were taken into consideration. Numbers of cycles were normalized to 10h of flight. The calculated RLS can be used for numerical simulations of crack growth or for laboratory tests. The results of such analyses and tests have great value because RLS is very similar to real usage profile.

(Research supervised by Andrzej Leski, Air Force Institute of Technology, Warsaw).

3.6 Flight Loads Acquisition for PZL-130 ORLIK TC-II Full Scale Fatigue Test

The aim of this work was to obtain the actual flight loads which will be used to determine a characteristic load spectrum for the Full Scale Fatigue Tests of PZL-130 ORLIK.

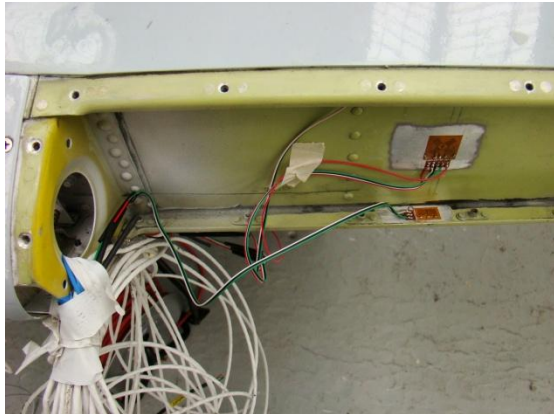
The flight loads measurement was carried out using strain gauges. The preliminary assumptions concerning the location and loads to be measured were delivered by EADS-PZL "Okęcie".



Sections and installed measurement points

The final measurement system consisted of 86 measurement points distributed at 13 different locations. Altogether 27 different loads were measured. The main objective was to measure the wings bending moments (especially in the root ribs). Moreover, the bending moments of the fin, horizontal stabilizer, fuselage

(in 2 sections) and landing gear were measured. Furthermore, torque in the root ribs and shear force in two inner sections of the wings were monitored.



Strain gauges installed in the middle wing section of the left wing on the front spar.

In order to determine the loads exerted on the aircraft structure by means of recorded strain signals, a calibration system was carefully designed and the calibration was scheduled before the planned test flights.

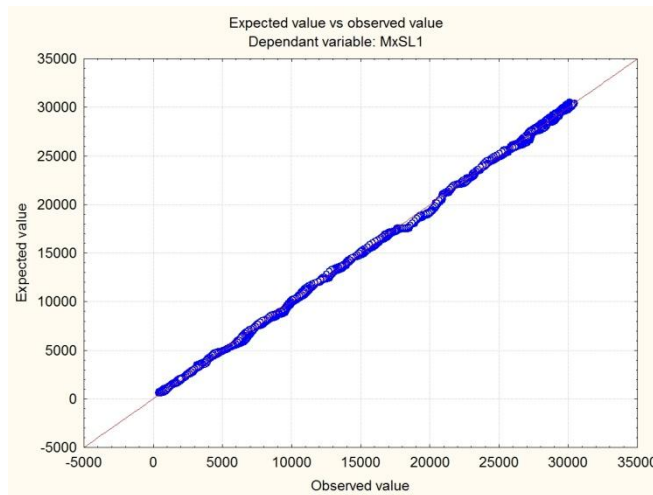
The calibration process was carried out in EADS-PZL "Okęcie". The general idea of the process was to exert known loads on the aircraft structure and simultaneously record the strains. The loads were applied by means of jacks and belts while force was constantly monitored with a dynamometer. To enable proper load distribution and to prevent any structural damage during the process, a number of special clamps were designed and manufactured.



Wing sensors calibration and clamps used for wing and fin loading

The level of excitation achieved with the available calibration methods was varying between 30-90% of operational loads for different loads. Assuming linear behavior of the structure within the whole flight envelope, such a range was sufficient.

Based on the values of forces applied and the strains recorded during calibration, the regression equations were determined.



Calculated value of MxSL1 (bending moment in root rib of the left wing) vs. real value measured with dynamometer

In order to determine the values of actual loads acting on the aircraft structure during flight it was necessary to perform a series of specially designed test flights. In addition to the recorded loads, it was necessary to gather coherent signals from the on-board flight recorder, e.g. velocity, pitch/yaw/roll angles etc.

The values of loads were calculated with the use of the determined regression equations. The obtained load history was the basis for determination of load spectrum for the Full Scale Fatigue Tests.

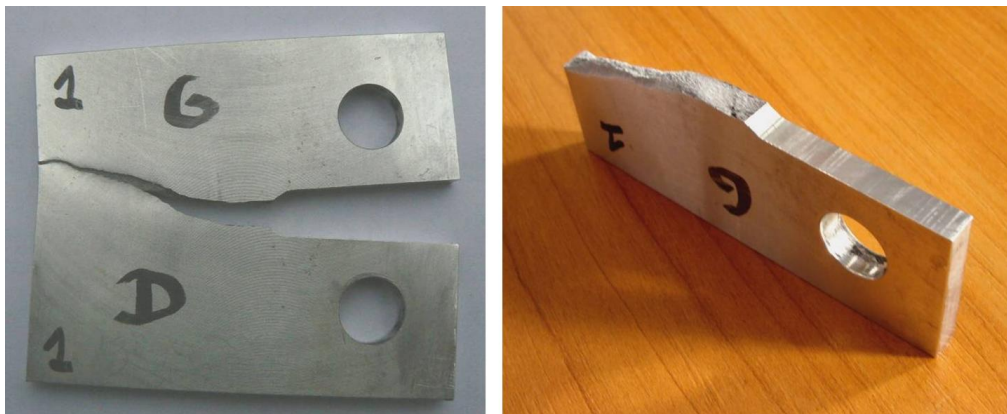
(Research supervised by Andrzej Leski, Air Force Institute of Technology, Warsaw).

3.7 PZL-130 ORLIK TCII Fracture Markers Solution for Full-Scale Fatigue Test

One of the purposes of the Full-Scale Fatigue Test (FSFT) is to provide information on the location and character of fatigue crack propagation. The FSFT usually produces several large cracks and many smaller ones. After applying loads, invisible cracks can be detected by means of Teardown Inspection (TI). In order to obtain information about crack history (crack growth rate, time of crack initiation and number of cycles), post-test Quantitative Fractography (QF) of crack growth is used. This method employs fracture surface markers, which are formed either naturally or by the intentionally developed load spectrum. The occurrence of markers depends on several factors: material, spectrum (loads, R ratio, intervals, peaks), environmental conditions, crack size and crack growth rate. The marker load strategies fall into five main categories:

- reordering the load spectrum
- overload additions
- underload additions
- constant amplitude (CA) groups
- combination of the above

One block of spectrum is made of 198 flights. It is equivalent to 200 flight hours. By reordering those flights, a block which should create a fracture marker was developed. Studies with the use of reordered load spectrum were performed on WOL-type aluminum alloy specimens.



WOL (Wedge Opening Load) specimen after test

The experiments aimed at finding the best fracture markers for FSFT of PZL 130 Orlik TCII, which should give us information about crack history.

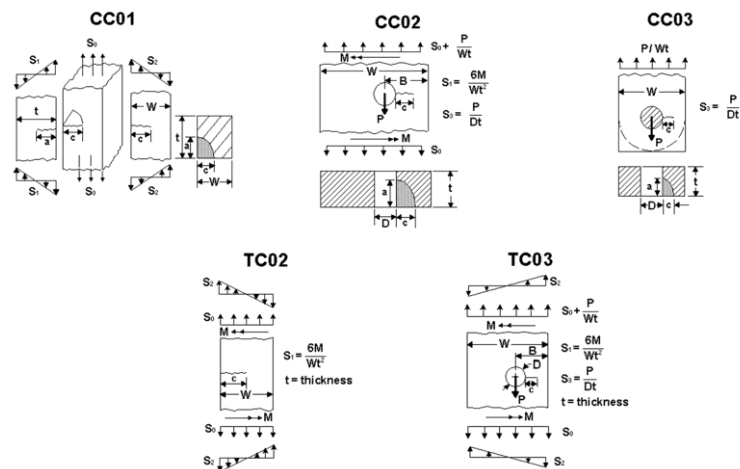
(Research supervised by Andrzej Leski, Air Force Institute of Technology, Warsaw).

3.8 The Cracks Propagation Calculations in the PZL-130 ORLIK Structure

The subject of the analysis was the critical elements of the PZL-130 ORLIK. The numerical crack growth analyses were performed using the NASGRO equation. The ORLIK aircraft are mainly used for the basic pilot training in the Polish Air Force. Each airplane is equipped with a digital flight data recorder. The record of more than 36000 flight hours is the basis for numerical analysis of fatigue life.

Operation of the aircraft according to the damage tolerance philosophy requires the determination of critical elements in its structure. Given the current lack of full scale fatigue tests of the PZL-130 ORLIK airframe, the finite element analysis was used to designate the critical elements of its structure. The elements of high positive stress level were selected. Only one load case (vertical acceleration – g load) was taken into account during the FE analysis. The consequences of this simplification were accepted.

The figure shows crack cases selected for the purposes of the analysis. Following the recommendations of the research methodologies and the NASGRO software instructions, crack models were selected according to the geometry of the critical element. The initial crack length applied in the calculations was 1.27 mm. Other dimensions were selected according to the measurements.



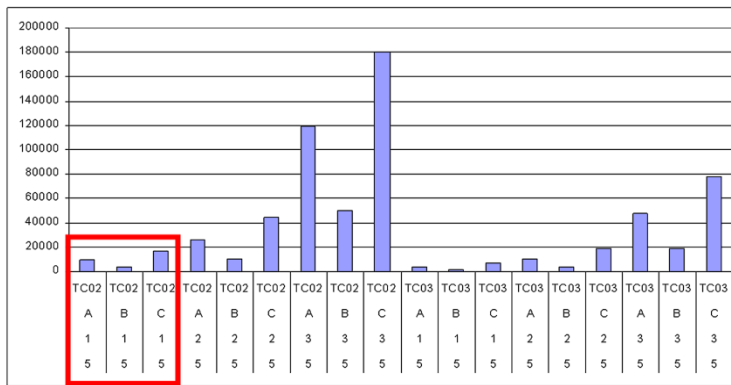
Crack cases selected for calculations

The Representative Loads Sequence (RLS) was developed for the trainer PZL-130 ORLIK. Recorded real flights were taken into consideration. The aim of developing representative load sequence (RLS) for the PZL-130 ORLIK was to obtain a load time history which would be the best approximation of loads acting on an aircraft structure during average flight. This load time history should be short enough to be used for numerical calculation or laboratory tests.

The single block of the RLS spectrum consists of 55 flight hours. The load values correspond to the recorded g load.

Based on information gathered on the critical location, spectrum and material properties, the fatigue life analysis was performed for twelve computational models. For all models, different spectra as well as crack cases were investigated. The first two calculation models were used to determine the fatigue effect of spectrum loads. The rest correspond to the critical elements selected for the analysis. To calculate the fatigue life and crack growth, the following load sequences were used:

- RLS Truncation 10%;
- FALSTAFF;
- RLS Truncation 10% (generalized Willenborg model).



Graphical representation of durability for the selected critical elements

Depending on a load spectrum chosen and a crack case, different results were obtained. So far, the operation of aircraft PZL-130 in Poland is less aggressive than the application of standard spectra would indicate. A more detailed analysis of sustainability requires a load sequence representing the local impact in a more accurate way. Critical elements defined using the global FEA model should be verified based on the full scale fatigue test.

(Research supervised by Marcin Kurdelski, Air Force Institute of Technology, Warsaw).

4. MATERIALS TESTING

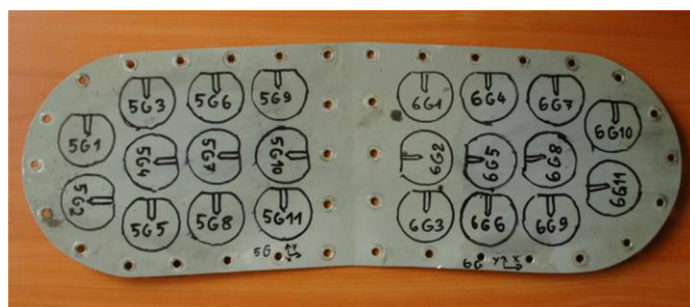
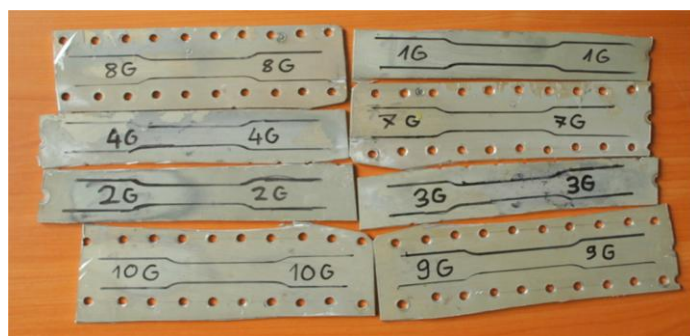
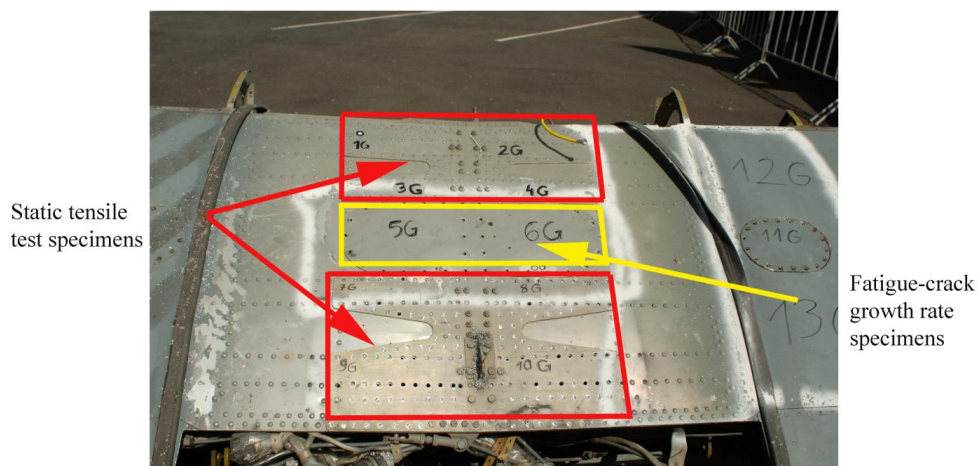
4.1 Investigations of Some Properties of Material Samples Taken from the Aircraft Withdrawn from Service

In the Air Force Institute of Technology the experimental tests were carried out to determine some specific properties of the materials used in the PZL-130 ORLIK aircraft structure. The samples were obtained from an aircraft removed from service. The following tests were conducted during the experiments:

- fatigue tests (crack propagation examination),
- static tests.

The analyzed material was taken from the central upper part of the aircraft wing. The experiment was conducted with the MTS machine with the 810.23 system.

Samples were collected from the wing of the PZL-130 TC-I.



Specimen No.	a_0	b_0	L_{0ve}	$R_{0,01}$	$R_{0,05}$	$R_{0,2}$	R_m	$A_{50\text{ mm}}$	E
	[mm]	[mm]	[mm]	[MPa]	[MPa]	[MPa]	[MPa]	[%]	[MPa]
5/09/1 (8G)	2,73	12,37	50,42	209	237	259	416	19,4	76700
5/09/2 (4G)	2,73	12,35	49,99	208	229	255	413	19,2	59900
5/09/3 (2G)	2,73	12,41	50,01	208	242	261	45	18,9	67800
5/09/4 (10G)	2,73	12,42	49,95	206	243	262	413	.*	79500
5/09/6 (1G)	2,73	12,40	49,87	222	242	260	413	18,5	61800
5/09/7 (3G)	2,73	12,29	50,23	232	250	268	418	.*	65400

The measurement results of static tensile test

* Failure outside the gauge length;

L_{0ve} - measuring range of video-extensometer;

$A_{50\text{ mm}}$ - set on the basis of video-extensometer indications.

The studies of fatigue crack growth rate were carried out on sixteen specimens (thickness 1.95 mm, equal to the thickness of the lid). The tests were carried out according to the test procedure PB-5/31 LBWM using the testing machine MTS 810.23. The frequency of cyclic loads was 15 Hz. The samples were tested with the cycles of the three values of the stress ratio $R = 0.1, 0.5$, and 0.8 . Each sample was tested at two stages - in the test range with decreasing ΔK (threshold propagation area of the curve $da/dN=f(\Delta K)$) and in the test of constant amplitude (critical area of the curve, to break the sample). To determine the crack length, the COD MTS extensometer was used. To measure the crack length, the vulnerability method was applied, and to determine the speed of crack propagation da/dN , the polynomial method was used. Test results are presented in the table below.

Specimen No.	m	C	N [cycle]	a [mm]	DK decreasing test			Constant Amplitude CA test		
					ΔK_{start} [MPa \sqrt{m}]	ΔK_{finish} [MPa \sqrt{m}]	N [cycle]	a [mm]	ΔK_{start} [MPa \sqrt{m}]	ΔK_{finish} [MPa \sqrt{m}]
5/09/10 (5G2P)	4,6880	1,708E-09	840119	12,4	14,8	4,3	1311589	22,6	4,7	27,1
5/09/11 (5G3W)	4,0064	1,00E-03	1203855	10,7	6,5	3,5	2658864	21,5	3,1	16,0
5/09/12 (5G4P)	2,9344	1,00E-03	2072501	8,9	2,7	1,5	4027008	18,3	2,1	6,8
5/09/13 (5G5W)	3,7289	1,247E-07	3430343	9,2	2,4	1,3	5318180	18,3	1,9	5,7
5/09/14 (5G6W)	2,8153	2,079E-07	2251292	8,7	2,7	1,6	4104500	18,4	2,2	7,1
5/09/15 (5G7P)	3,5479	5,569E-08	1258899	11,3	6,5	2,1	2441518	21,8	2,8	13,9
5/09/16 (5G8W)	4,5524	1,796E-09	804594	12,5	15,2	4,5	1218128	22,4	5,3	27,0
5/09/17 (5G9W)	4,3706	5,667E-09	877972	13,5	14,1	5,3	1125009	21,6	5,3	19,7
5/09/20 (6G1W)	2,6219	2,398E-07	2490962	9,0	2,7	1,5	4618199	18,8	2,0	6,9
5/09/20 (6G1W)	4,2704	7,181E-09	1171257	14,3	14,7	3,4	1234447	22,1	5,7	7,9
5/09/20 (6G1W)	4,0501	1,500E-08	985100	13,4	14,4	3,1	1104883	21,6	5,0	18,2
5/09/20 (6G1W)	3,7797	5,449E-09	934667	13,9	14,9	3,9	1375344	22,0	4,7	33,8
5/09/20 (6G1W)	3,8440	5,587E-08	836681	11,2	6,3	2,1	1685247	21,0	2,7	11,5
5/09/20 (6G1W)	3,1478	1,349E-07	2081698	8,5	2,7	1,7	4427581	18,5	2,1	7,3
5/09/20 (6G1W)	4,4192	5,206E-09	830914	13,2	14,3	4,9	1100788	22,0	4,9	19,7
5/09/20 (6G1W)	3,8739	2,641E-08	1196023	10,6	6,5	2,5	2001889	21,2	3,3	15,2

The presented results are the first step in examining the impact of the operation of the PZL-130 ORLIK on the properties of the materials used.

(Research supervised by Sylwester Kłysz, Air Force Institute of Technology, Warsaw).

4.2 Predicting Fatigue Crack Growth and Fatigue Life under Variable Amplitude Loading

This work focused on a probabilistic approach to the description of fatigue crack growth and fatigue life estimation of a component subjected to variable amplitude loading.

A probabilistic model is proposed. The reasons for applying the probabilistic approach are as follows:

- inhomogeneity of the real material,
- scatter of mechanical properties of the material,
- randomness of the cracking process,
- technological conditions (quality of manufacturing).

It is required that the model and the real object are physically identical as regards the time and point of crack initiation, crack propagation period and fatigue lifetime of a component. Generally, service loading contains a wide spectrum of stress cycles such as base line cycles, overloads and underloads, which appear in different order. The application of single or multiple tensile overloads causes significant decrease in the crack growth rate for a large number of cycles subsequent to overloads. This results from the compressive residual stresses acting in the plastic zone ahead of the crack tip. The application of compressive underloads has a detrimental effect on crack initiation and crack growth. The crack growth rate shows increasing trend and fatigue life will be reduced.

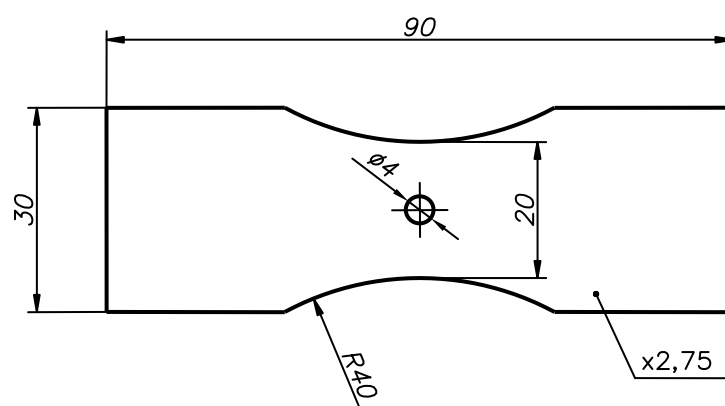
In order to calculate the retardation effect on the crack rate due to overload-underload cycles, the improved Wheeler model known as the Willenborg model was applied. Both these models are based on the assumption that crack growth is controlled not only by the plastic zone but also by residual deformation left in the wake of the crack as it grows through the previously deformed material.

The probabilistic model developed in the work facilitates a simplified description of fatigue crack growth under variable amplitude loading and the estimation of fatigue life. A finite difference equation with the coefficients originated from the Paris formula, which models the crack growth dynamics, is fundamental for the description. The characteristic features of crack growth under overload-underload cycles existing under exploitive loading were modelled using the modified Willenborg retardation model. The method has a good confirmation by experimental research of crack behaviour and fatigue life estimation for the aeronautical aluminium alloy sheet 2024-T3 subjected to variable amplitude load program. This method needs an extension over the crack initiation period.

(Research supervised by Dorota Kocańda, Military University of Technology, Warsaw).

4.3 The Analysis of a Fatigue Crack Propagation in the Elements of Aluminum Alloy D16CzATW with a Notch in the Form of a Cylindrical Hole

The work focused on the fatigue resistance of specimens made from the aluminum alloy D16CzATW. For the purpose of the research, flat specimens with notches in the form of cylindrical holes were manufactured by drilling and reaming. The research was carried out under the conditions of constant-amplitude bending at the stress ratio of $R = -1$. The results obtained from the research were compared with fatigue resistance of specimens with calibrated holes and specimens without notches. Fatigue resistance was determined for plated specimens and those without a protective layer. Very large differences in fatigue resistance have been obtained. This can be explained by the negative effect of the brittle plate layer on the fatigue crack initiation. A complicated fracture mechanism was noted, in which micro-mechanisms of brittle and plastic fracture were appearing at different stages of fatigue crack propagation.



Specimen for a fatigue tests.

Fatigue resistance graphs were obtained for specimens with a drilled and reamed hole, also for specimens with two-sides plated and without a plate layer. The results obtained were compared to those obtained for the specimens without a notch or a calibrated hole.

Good repeatability of results was obtained, resulting from high microstructural monogamy of alloy D16CzATW. The fatigue resistance of a specimen with a drilled and reamed hole was 3-4 times lower than that of a specimen without a notch. It has been established that calibration beneficially influences the fatigue resistance of a specimen. In the case of specimens subjected to calibration at the degree of $k = 3,25\%$ in relation to specimens with holes that were not strengthened, fatigue life increased by between 15 % and 35 % depending on the level of bending stress amplitude. Also, an unfavourable effect of plate layers on the fatigue life was observed. The fatigue resistance of specimen with a drilled and reamed hole after the removal of the plate layer increased from 27% under bending stress amplitude $\sigma_a = 180$ MPa to 140 % under $\sigma_a = 135$ MPa in relation to plated specimens. The plate layer is the source of a great number of surface microcracks, which in turn accelerate the fracture process.

The cause of such material behaviour was investigated by the analysis of micro fracture mechanisms. Microfractographic analysis of fracture surfaces detected numerous signs of brittle and quasi-brittle fractures under small part of plastic deformation. An increase in cracking depth was accompanied by the intensification of plastic deformation. The formation of multi-directionally oriented systems of fatigue striations and a great number of secondary cracks were observed.

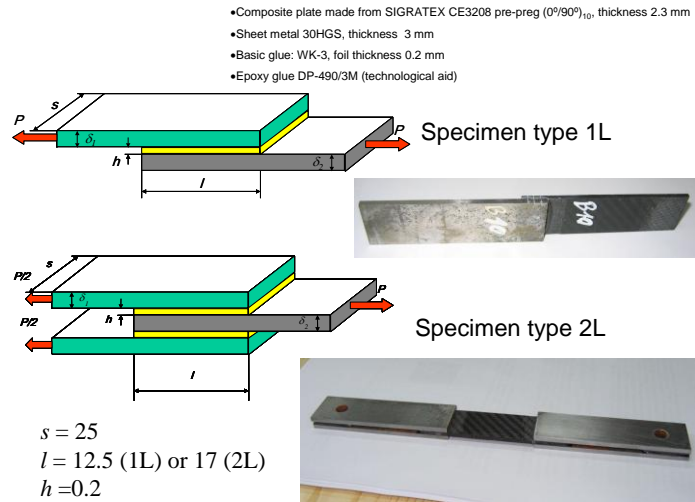
(Research supervised by Volodymyr Hutsaylyuk, Military University of Technology, Warsaw).

5. JOINTS

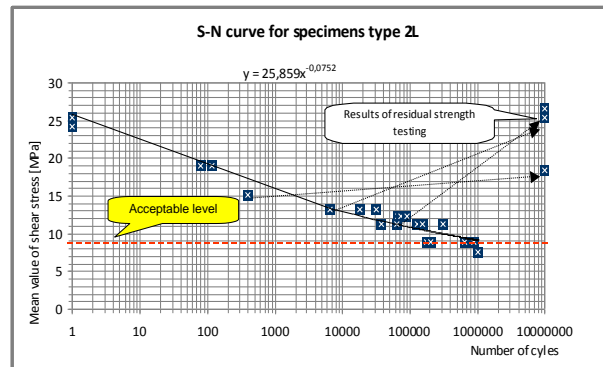
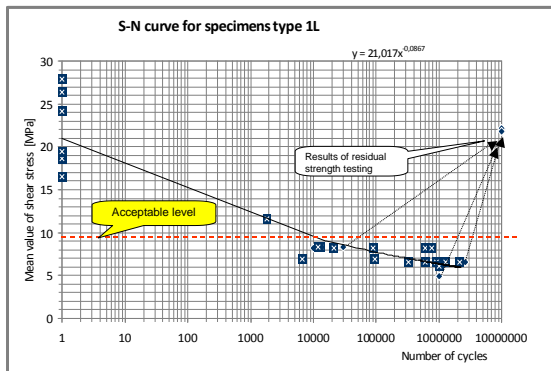
5.1 Investigation into Fatigue Behaviour of Metal-Composite Glue Connection

The experimental investigations into fatigue properties of metal and CFRP-composite glued joints were performed at the Warsaw University of Technology.

The object of the investigation was adhesive joints between metal sheets made from iron alloy 30HGS and CFRP orthogonal reinforced sheets made from 10 layers of SGRATEX CE3208 pre-preg. The main adhesive was the WK-3 glue applied in the form of 0.2 mm thin foil. Two types of specimens were prepared and tested: single-lap joints and double-lap joints.



S-N curves for both kinds of those specimens were developed.



Besides on the fatigue life of the glued joints, the investigations focused on the NDT tests regarding damage propagation inside the glue-connection. Several C-scans were made at different stages of fatigue testing. It has been found that the damage occurs almost equally in the whole volume of the glue layer (contrary to the expectation following from the physical model of the glue-connection internal loading).

The following features were observed for the glued joints considered:

- Double-lap glue joints reveal about 100 times higher fatigue life than single-lap glue joints.
- The fatigue process takes place almost equally in the whole area of the glued joints.
- Thermal gradient increases with fatigue advancement. This could be used as an important parameter for diagnostics purposes.

(Research supervised by Mirosław Rodzewicz, Warsaw University of Technology, Warsaw).

5.2 Experimental and Numerical Study of Stress and Strain Field around the Rivet

The presented work was carried out under the IMPERJA project (Eureka initiative, the project E3496!). The goal of the IMPERJA project was to increase the fatigue life of riveted joints as well as to improve fatigue life estimation methods for such joints. The project included experimental and numerical analyses of the stress and strain system around the rivet as well as the impact analysis of joint geometry and squeezing force. The investigation concerned sheets and rivets used in the Polish aerospace industry.

The work focused on the determination of stress and strain field induced during riveting and FEM modelling of this process. Stress and strain measurements during riveting allow for better understanding the phenomena that occur during this process and determining stress and strain field which exists in the joint after riveting. The results will be also used for validation of FEM models.

Stress and strain measurements were carried out with the X-ray diffractometer and strain gauges on the sheet surface near the driven head. The investigation concerned sheets and rivets used in the Polish aerospace industry. The measurements for two types of rivets; the brazier rivet (BN-70/1121-06) and the rivet with a compensator (OST 1 34040-79 1), as well as the FEM analyses, were performed. Bare sheets made from 2024 T3 aluminium alloy with the nominal thickness of 1,27 mm and rivets with the diameter of 3 mm and 3,5 mm made from Polish aluminium alloy PA25 were used.

The effect of squeezing force as well as the rivet type on stress and the strain system was investigated.

Two types of strain gauges were used. The strip miniature gauges with the gauge length of 0,51 mm were located outside the driven head and worked during the whole riveting process. The micro strain gauges with gauge length of 0,38 mm were applied very close to the rivet hole, in the area which is under the driven head after the riveting process. The gauges recorded strain up to the point when they were destroyed by the driven head.

The measurements results were compared with the FEM results.

Higher stress and strains after the riveting process were found for higher squeezing force and for the rivets with compensators.

The literature and the FEM calculations indicate the presence of the high stress and strain gradient near the rivet hole. The XRD measurements covered the region on the boundary or outside the high gradient stress area. This was the reason for the strain gauge measurements. The high strain value near the rivet hole was proved. The presence of compressive tangential strains in this region was not experimentally confirmed. The „S” shaped plot of radial strain for the rivet with a compensator was recorded. A similar shape of strain plots was obtained by other researchers but this phenomenon has not been explained yet.

Good correlation of FEM calculation with the XRD and strain measurements was obtained. Numerical results indicate positive influence of the rivet with a compensator on the stress system after riveting in sheets. Compressive stresses are present also in the sheet on the manufactured head (more uniform stress distribution through thickness). The area of compressive stress presence is larger in comparison with the brazier rivet. The range of plastic zone is also significantly larger. The benefits of using the rivets with compensators were confirmed by the fatigue test results.

The work will be presented by Wojciech Wronicz during the 26th ICAF Symposium – Montréal, Canada, 1–3 June 2011.

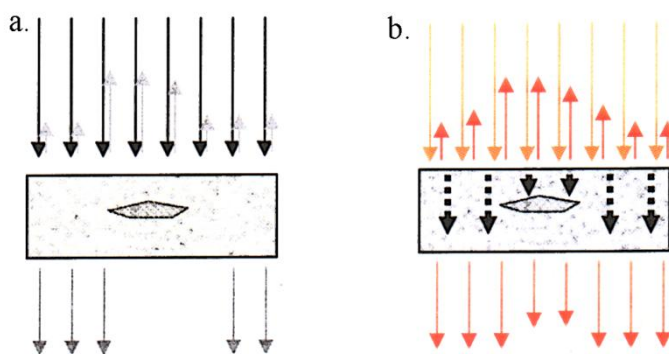
(Research supervised by Jerzy Kaniowski, Institute of Aviation, Warsaw).

6. NON-DESTRUCTIVE TESTS AND STRUCTURAL HEALTH MONITORING

6.1 Diagnostics of Composite Aircraft Structures using Non-Destructive Tests with Thermographic, Ultrasound and Acoustic Methods

Control and constant supervision over the technical condition of composite aircraft structures are necessary for the safety of exploitation. Even small damage of the composite aircraft structures, caused mainly by heavy loads and changeable atmospheric conditions, will weaken the structure and may lead to serious accidents. Bearing this in mind, periodical controls using non-destructive tests are conducted. The most popular methods widely used in aviation are those based on ultrasound and acoustic phenomena occurring in examined structures. The ultrasound method consists in emitting ultrasound waves from a transmitter into the material. The material has defects (borders of connections, delaminations) which are the reflectors from which the wave reflects and comes back to the transmitter head. Examination of this phenomenon is based on observing the amplitude volume and direction changes of ultrasound waves and on the time measurements of the wave passing through the examined material. Other techniques used for detecting defects in composite structures are ultrasound resonant techniques based on the measurement of resonant vibrations of a given material. Continuous waves introduced into the material are gained or damped. Amplitude and phase of vibrations on the material surface depend on the flexural modulus and thickness of the material under the head. Acoustic impedance is another physical phenomenon used (method-MIA). The method is based on the resistance (dampening) measurement of acoustic waves with a specific volume of the examined material.

The above-mentioned non-destructive tests are not the only techniques of examining composite structures. Due to improvement of composite structures, engineers are forced to implement the latest examination methods. One of these methods is pulsed thermography. This method consists in even activation of the structure by thermal pulse and monitoring changes in temperature distribution of the examined surface, while it is cooling down, by means of a TV camera. Defected areas lose heat much more slowly and therefore they are characterized by temperature higher than that of the areas free of material defects.



Presentation of physical phenomena similarities in the examined material:

a) dispersion of ultrasound waves;

b) dispersion of thermal wave.

This work presents examination results of individual techniques demonstrated on composite samples of the laminar and sandwich

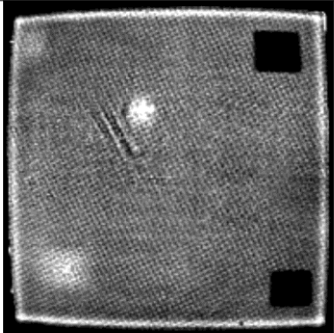
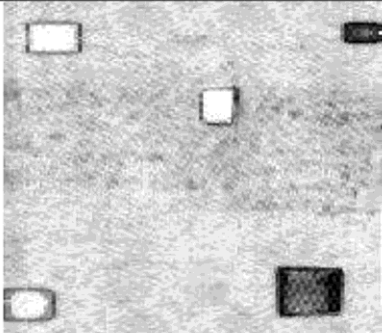

structure as regards damage characterized by ungluing of glued joints and delamination. Defects detection levels were verified depending on the sizes of the defects. The following presentation of selected methods aims at highlighting their respective advantages and disadvantages as well as the optimal ways of applying them in normal conditions.

Research materials and equipment

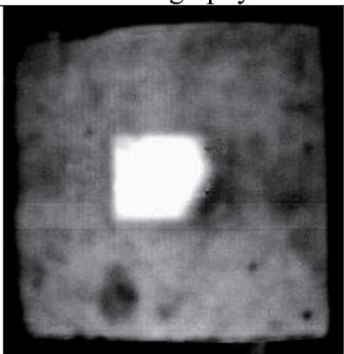
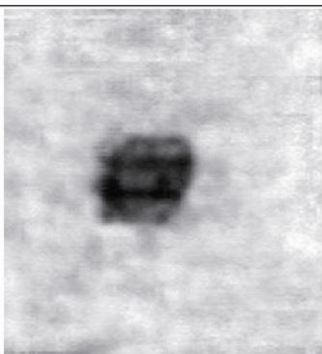
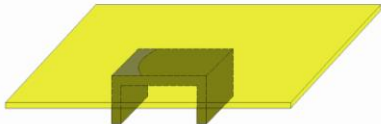
Typical materials used in aviation were used in the examinations conducted. Composite samples of the laminar and sandwich structure were used for conducting the examinations.

The automated MAUS system, equipped with exchangeable heads, and the presentation of results in C mode-Scan were used for controlling composite structures with acoustic and ultrasound methods. The EchoThermSystem equipped with xenon lamps and a professional TV camera was used as the research equipment based on pulsed thermography.

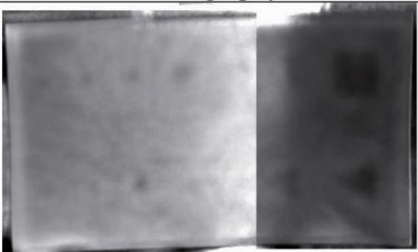

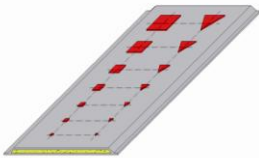
- Composite plate reinforced with carbon fibres.

Pulsed thermography method	Ultrasound method	Sample
 <p>Examination time 2s</p>	 <p>Examination time 40s</p>	

- Plate manufactured on the basis of glass fibres of the laminar structure.

Pulsed thermography method	Resonant method	Sample
 <p>Examination time 5s</p>	 <p>Examination time 40s</p>	

- Composite plate with foam core reinforced with carbon fibres.

Pulsed thermography method	Acoustic impedance method; MIA	Sample
 <p>Examination time 60s</p>	 <p>Examination time 50s</p>	

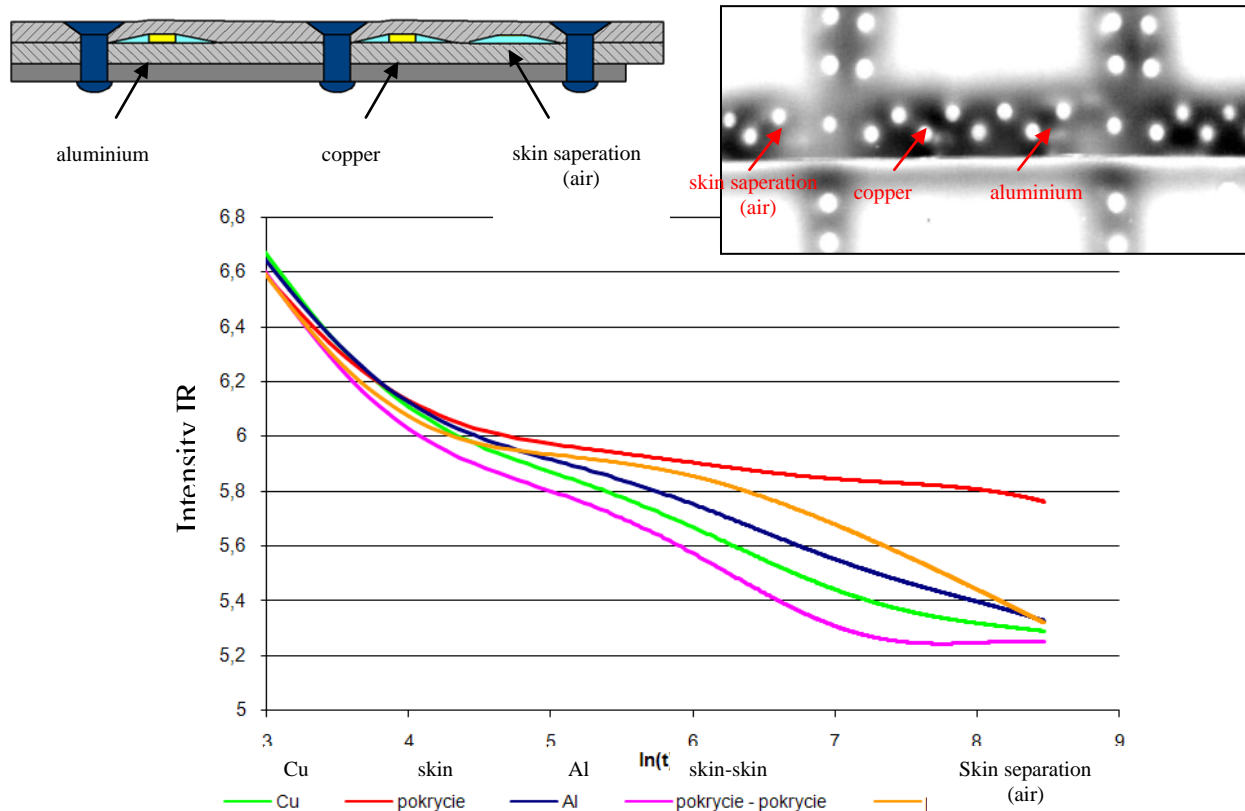
The aim of the conducted tests was to estimate the flaw detection rate in composite structures and glued joints. Not all methods applied allow detection of material defects in the examined structure. The problems concern the inspection of the sandwich structure e.g. foam core, which has muffling characteristics eliminating the application of the ultrasound method, whereas the method of acoustic impedance delivers information about the internal structure of the examined material. The technique of pulsed thermography allows acquiring information about the imperfections of the structure in a wide range of composite materials across a wide

range of surfaces in a relatively short time (a few seconds) compared to acoustic and ultrasound methods, for which the time of examination is longer and dependent on the size of the scanned surface. Thermographic images (thermographs) reflect the physical condition of examined samples and internal flaws in the material can be detected, however, their geometry and location influence the accuracy of the method. For the interpretation of the examination results, the special software can be used in order to increase the accuracy of the surface analysis by means of differentiation of the first and second degree of temperature curves at a given point.

(Research supervised by Krzysztof Dragan, Air Force Institute of Technology, Warsaw).

6.2 Analysis of the Possibility to Assess the Occurrence of Hidden Corrosion in Lap Joints using Active Thermography

The work concerns the NDT technique of pulse thermography used for objective diagnosis of the riveted lap joints construction. The degradation of materials manifesting as corrosion is inherent in the process of aircraft operation. One type of corrosion is galvanic corrosion occurring in the overlap joints (known as hidden corrosion). As a result of the potential difference between the two layers of the aluminum alloy skin, oxidation of the material occurs, producing corrosion products in the form of oxide compounds characterized by heat properties different than those of the base material. This allows their detection with thermographic methods. Preliminary tests were carried out on the object with riveting joints. Solids with other thermal parameters in relation to the base material (aluminium alloy) were introduced to lap joints. Solids cause disruption in homogenous intensity of infrared radiation emission on the surface of the tested object. The thermograph and the diagram illustrating the surface intensity of infrared radiation during cooling is presented below.



Thermograph of the sample tested and a diagram illustrating the surface intensity

The preliminary results obtained with the pulsed thermography method show the usefulness of the selected technique for the evaluation of hidden corrosion in aircraft structures. With the method used, we can easily and quickly check the quality of paint coating when applied and its condition during aircraft operation. The infrared technique also offers the opportunities for detecting material inclusions of different thermal properties, which are between two materials. As a result, a different infrared radiation wavelength is achieved in the area where material compounds of different thermal parameters are present.

(Research supervised by Krzysztof Dragan, Air Force Institute of Technology, Warsaw)

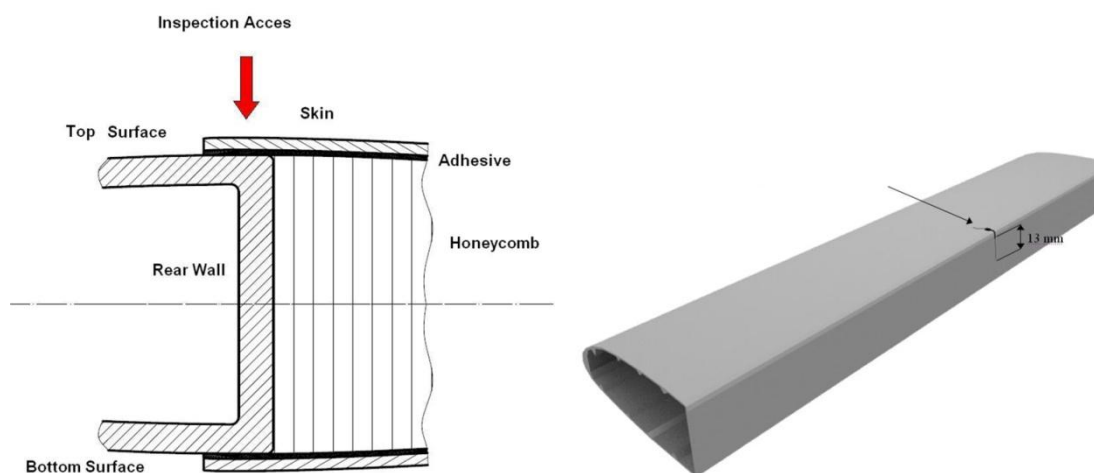
6.3 Structural Health Monitoring Approach to the Aerospace Structures

In recent years there has been observed an enormous growth of interest in continuous and periodical condition monitoring of civil and aerospace structures with the use of Structural Health Monitoring techniques (called SHM). Such systems use ‘*physics*’ of NDT for data acquisition with the use of so called “smart layers”. These “smart layers” are based on sensor networks distributed in the structure of the object under monitoring. Such an approach enables condition monitoring with limited human interaction.

A few works aimed at the monitoring of the structures have been conducted by the Air Force Institute of Technology.

Methodology of Crack Growth Analysis

One of the important examples of the monitoring necessity is rotorcrafts. In the helicopter main rotor blade, there occur fatigue cycle phenomena which may lead to critical failure. Monitoring such failure modes is crucial from the safety and durability of the structure point of view. It is possible to describe the critical damage areas, which is very important from the maintenance point of view. Monitoring such areas may be performed with the use of the classic NDT approach. Modern maintenance philosophies require a more advanced approach to structural integrity monitoring such as the multimode NDE approach.



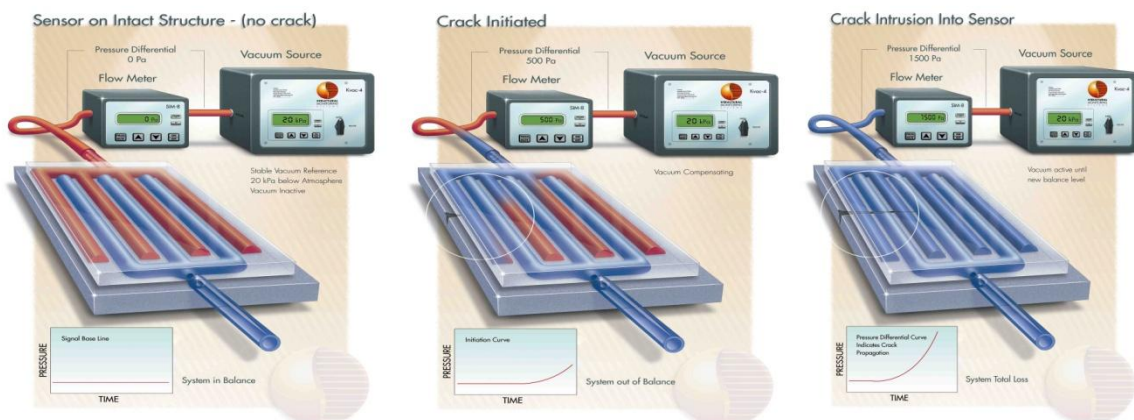
Geometry for inspection

During R&D work conducted in the Institute (AFIT) for the structure assessment, conventional NDT methods have been used (ultrasonic and eddy current). These techniques, however, do not allow for rear web inspection. This is why monitoring techniques which use the embedded sensors (CVM™ and PZT sensors) have been applied.

For the blade monitoring, the PZT sensors were used. These sensors enable generating elastic waves in the blade structure. Based on the wave propagation analysis as well as the phenomena associated with reflection and mode conversion, the signal analysis was performed. Such analysis enables damage detection and damage description. The advantages of this method are following: possibility of signal transmission for further distances, sensitivity to changes in the structure integrity.

The limitations are connected with the interpretation of the data and the necessity for the signal modeling. Also, difficulties connected with boundary interaction of the wave and mode separation may appear. From that point of view, the necessity of the modeling must be taken into consideration.

The technique called CVM™ is connected with the crack monitoring. This technique is simpler than wave generation. Monitoring is based on local crack detection. Sensors consist of multiple measurement galleries. There are two channels in each sensor (connected to the vacuum generator and ambient pressure). Damage localization is connected with the vacuum generation in the measurement galleries. The principle of work is presented in the figure below. Depending on the crack length, crack orientation and sensor shape, pressure variations indicate crack propagation under the sensor, which means there is a possibility for crack length estimation.



Principle of work of the CVM™ system

The main advantages of the method are the following: possibility of fast and indirect measurement, lack of electrical cabling and on-line monitoring. The disadvantages are connected with the necessity of structure monitoring in “hot – spot” locations and for that reason global monitoring is not possible.

Monitoring of the Centrifuge for Pilots

The structure of the centrifuge is similar to the structures used in the aerospace solutions. In that case it is possible to determine: spars and ribs, skin and fasteners. Also, there is a similarity connected with the materials and geometry. Based on that, it is possible to use monitoring techniques similar to those used in aerospace. For such structures, the classic

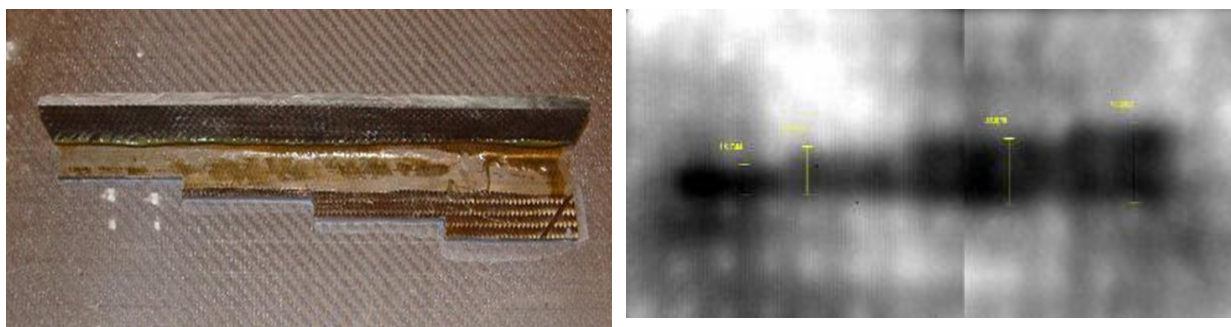
approach with the use of NDE techniques may not be efficient. Based on the AFIT experience of conducting inspections, the critical “hot spots” have been determined.

The CVM™ sensors as well as strain gauges were applied. At present, the application is used for periodical monitoring. Right now, there are being determined work packages which may enable system integration with the centrifuge data acquisition system as well as works connected with data comparison from CVM™ sensors with the NDE inspections.



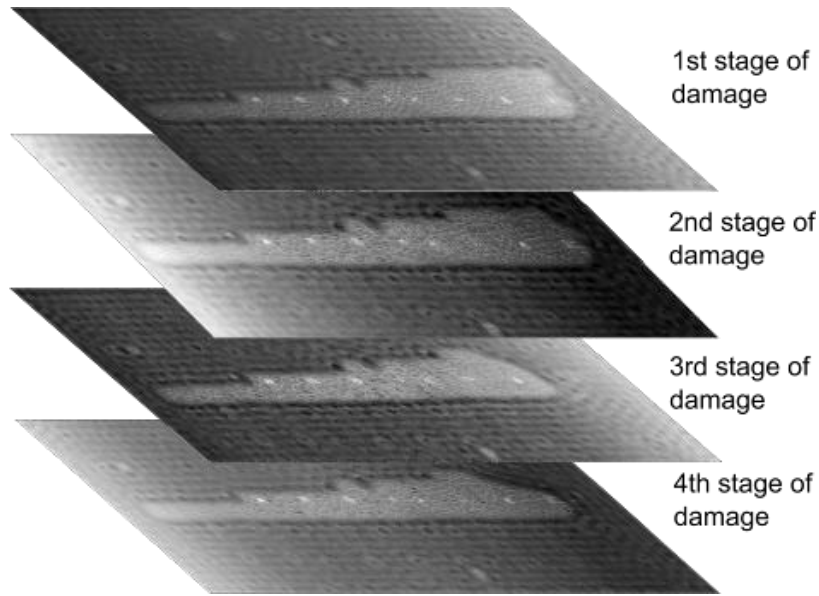
Bonded joint monitoring of the composite aerospace structures

The work focused on the bonded joint monitoring. Based on information about typical ultralight aircraft structures, a specimen modeling the wing of the small aircraft has been designed. The specimen contains the sandwich skin (CFRP with foam core). Under the skin, the stiffener, which is a model of the spar, has been bonded. This structure is characterized by strong attenuation of acoustic (ultrasonic) signals. Tests carried out on similar structures have shown the effectiveness of the MIA method.



Specimen of the wing skin (left) and thermography results (right)

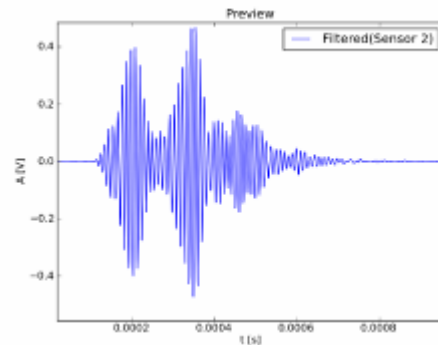
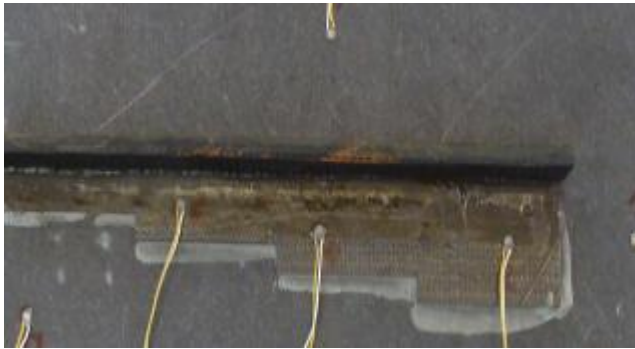
The propagation of damage is illustrated below in the form of C-scan:



Propagation of disbond

The damage growth was investigated with the use of the MIA method. However, some of the materials may be difficult for the inspection with the use of NDT. The signal attenuation and structure complication may be a challenge for the NDT. Moreover, the inspection of large scale structures is time-consuming. For these reasons, the application of SHM may be interesting.

The specimen was instrumented with the piezo sensors array and analyzed with the acousto-ultrasonic approach.



PZT sensors layout and example of generated signals

For such a layout of the sensors, the disbond growth may be efficiently monitored.

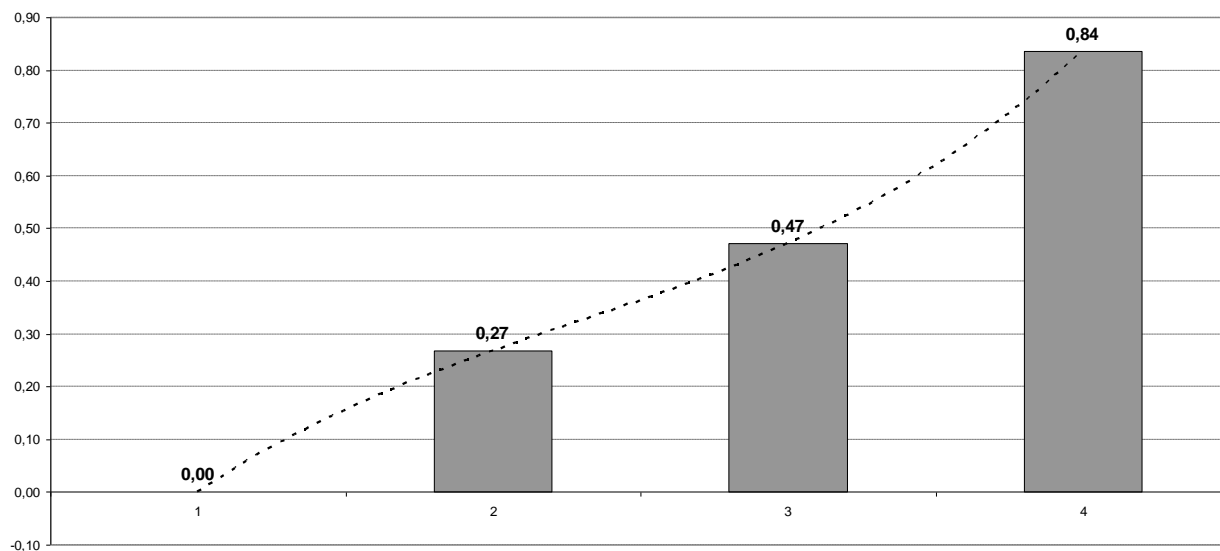
Damage presence and damage development may be described with the Damage Index. Based on the experience gathered during the previous research project, the following formula for the Damage Index was used:

$$DI = 1 - \frac{\int_{u_0}^{u_1} Wf_t(u, s_o) du}{\int_{u_0}^{u_1} Wf_b(u, s_o) du}$$

Where: $Wf_t(u, s_o)du$ – energy of the signal from the damage;

$Wf_b(u, s_o)du$ – energy of the signal from the so called baseline.

If there is a non damage condition, the index is equal to 0. If the damage develops, the Damage Index is equal to a value higher than 0 but never reaches a value greater than 1.



Results of the damage index development for the experiment

(Research supervised by Krzysztof Dragan, Air Force Institute of Technology, Warsaw)

7. THE SYNTHETIC DESCRIPTION OF THE RESULTS, SCIENTIFIC ACHIEVEMENTS AND PRACTICAL APPLICATIONS

THE EUREKA INITIATIVE, THE PROJECT IMPERJA, E3496¹, IMPROVING THE FATIGUE PERFORMANCE OF RIVETED JOINTS IN AIRFRAMES¹

(By Jerzy Kaniowski)

Consortium Members:

Institute of Aviation Poland, Coordinator

Polish Aviation Factory - PZL Mielec

AGH - University of Science and Technology, Faculty of Mechanical Engineering&Robotics

UTP - University of Technology and Sciences in Bydgoszcz - Faculty of Mechanical

Eng., Dept. of Machine Design

WAT - Military University of Technology, Inst. of Materials Science and Applied Mechanics,

Dept. of General Mechanics

Stresstech Oy in Finland

Evektor Spol. S.R.O. Czech Republic

The goal of the project was to increase the fatigue life of the riveted joints, which leads to an increase in the aircraft service life, a smaller number of inspections and, as a result, lower operating costs for an aircraft. It has been demonstrated that this goal can be achieved by the analysis and optimization of the riveting process as well as by improving the fatigue life prediction methods (crack initiation and propagation).

All activities in the aerospace area are subjected to regulations. Significant formal changes have taken place in the aircraft design regulations in recent years. The European Aviation Safety Agency, established in the EU in 2002, introduced the *Certification Specification (CS)*, which contains *the* airworthiness code and acceptable means of compliance for the particular types of an aircraft. In 1997, in the US, the *Code of Federal Regulations (CFR)* was introduced relating to all areas of life including politics, law and economy. The aircraft design regulations are contained in the *Title 14 CFR*. The merit changes have taken place too e.g. the introduction of the *damage tolerance* as a basic methodology for commuter aircraft. The standard recommended by the *Certification Specification* and the *Title 14 CFR* are the American Society for Testing and Materials (ASTM) standards for material tests and the NASM1312 *Standard Practice. Fastener Test Method* standards for riveted joint tests.

The strong correlation between the service life and Direct Operating Costs (DOC) of the aircraft has been proved with the calculation carried out according to the methodology described in the book *Airplane Design* by Jan Roskam, part 1, 8. For example, extending the service life of the M28 Skytruck airplane from 8 000 to 32 000 hours could decrease its DOC to 47%, which should directly affect the aircraft price.

The IMPERJA project consist of two parts: basic and applied research.

The program of basic research was developed based on the wide literature available. The authors assumed that experimental and theoretical results should be valuable for the aircraft life estimation and manufacturing. Some previously examined research topics were repeated for sheets and rivets materials used in the aerospace industries in Central Europe.

A wide range of tests of the materials used in the riveted joints were conducted. These covered monotonic and fatigue (high- and low-cycle) tests as well as examinations of fatigue

¹ <http://www.eurekanetwork.org/project/-/id/3496>

crack growth. Two sheet materials (D16AT [and its variation D16CzATW] and 2024-T3), two types of anti-corrosion layer (alclad and anodised) and three rivet materials (PA24, PA25 and 2117) were compared. The tests performed enabled the comparative analysis of the above mentioned aluminium alloys used in the Polish aerospace industry (D16, PA24 and PA25) as well as two types of alloys used in the West (2024 and 2117).

The Portevin-Le Chatelier effect has been observed in the monotonic tests, especially for the specimens cut lengthwise to the rolling direction. This phenomenon was also visible in the elevated temperature tests (for the range of 25°C to 200°C). During the tests, complementary methods were used: the passive IR-thermography and the acoustic emission. This allowed for widening the knowledge about the investigated materials. Moreover, the tear and shear tests for various squeezing forces were carried out.

The methodology of the residual stress measurements for the riveted joints with use of the XSTRESS3000 X-ray diffractometer (XRD) was developed. This methodology allows eliminating the effect of the driven/manufactured head shadow on the measurements. An extensive program of residual stress measurements near the rivets was carried out. The measurements concerned specimens with various types of rivets used in the PZL Mielec (countersunk and brazier, standard and with a compensator) and various riveting technologies (normal and NACA). The specimens were riveted with the force control. It has been demonstrated that rivets with compensators and the NACA technology cause higher compressive tangential stress on the manufactured head side. This significantly affects the fatigue life.

The strain measurements on the sheet surfaces near the driven heads during riveting process was carried out with strain gauges. The riveting processes were performed on the testing machine with the force control. The measurements were made for a 90° countersunk head rivet and a brazier rivet (standard and with a compensator). S-shaped² plots of strain as a function of squeezing force were recorded. This phenomenon was the most visible for the countersunk rivets. A similar shape of strain plots was presented by G. Li at all in paper [1].

The analysis of the Müller and Hart-Smith results [2,3] has indicated that when a 1,42-time increase in the squeezing force (from 12 to 17 kN, D/d parameter from 1,2 to 1,5; where D-driven head diameter, d-rivet shank diameter) resulted in a twofold increase in the fatigue life, then a three-time increase in the squeezing force (from 12 to 36 kN, D/d parameter from 1,2 to 1,7) resulted in an eleven-time increase, and in case of riveting with the NACA technology, even an eighty-time increase in the fatigue life. The magnitude of the life increase suggests that the change of the joint formation mechanism has taken place. The working hypothesis has been assumed that, for the significant increase in the squeezing force, the plastic strain level necessary for adhesive joint formation (cold welding) has been reached. The destruction of an adhesive joint requires significantly higher force than that needed for the destruction of a mechanical joint. Consequently, the fatigue life of a riveted joint is much higher. The specimens with various types of rivets (countersunk and brazier, standard and with a compensator) and different riveting technologies (normal and NACA) were prepared at a wide range of squeezing forces. The standard anodised layer was removed in some rivets. So far investigations have demonstrated the existence of punctual and continuous joints on some part of the contact surface between the rivet and the sheet for the countersunk rivet with the anodised layer removed, for D/d=1,7. It is not certain, however, whether cold welding occurred in these joints.

The extensive FEM analyses of the riveting process were carried out. These covered static (with force control) and dynamic riveting. The axisymmetric and solid models were used. The material and geometrical nonlinearity was taken into account. The Stick-Slip Coulomb

² Reversal strain signal

friction model (one of five implemented in the MSC MARC software) was chosen for the calculations, based on the numerical analyses. The materials models were developed based on the monotonic test. The results obtained from the axisymmetric and solid models were very similar, but the calculation time was incomparably shorter for the axisymmetric model. For frequently repeated analyses (e.g. optimization of the riveting parameters), axisymmetric models are the most convenient. The plots of radial and tangential stress and strain after riveting are consistent with the results obtained by Müller [2] as well as with the XRD and strain gauge measurements. Acceptable correlation of strain progress during riveting process in the calculation and the experiment (strain gauge measurements) has not been obtained, especially for tangential strains.

Rivets with compensators improve the transfer of the rivet material into the rivet hole and provide better hole filling in the sheet at the manufactured head side (the compensator causes a twofold increase in radial expansion of the rivet hole in the sheet, which means that radial displacements of the hole in both sheets are at the same level). Increasing the squeezing force value causes enlarging the plastic zone near the rivet. A considerably bigger effect can be obtained by restricting the driven head diameter (with the riveting set equipped with the ring) without changing its height. This causes a significant stress increase in the sheet, higher squeezing of the rivet shank in the hole and a more uniform stress distribution across the whole thickness of the sheet on the driven head side. Unfortunately, the difference between radial expansion of the hole in both sheets also increases, while the most desirable effect is when the radial expansion is at the same level in both sheets.

The numerical simulation of the riveting process has revealed monotonic decrease in average contact stress and equivalent stress caused by an increase of backlash between the rivet and the hole edge (within the range indicated in the riveting manual). Moreover, in the case of the countersunk rivet, with high backlash, the filling of countersunk part of the hole is not sufficient, as is indicated by low contact stress values in that area.

Standard and reversed dynamic riveting techniques were compared by means of numerical simulations. Reversed riveting (riveting hammer on the side of the manufactured head with a compensator) is more appropriate since, in the case of standard riveting, at the first stage of the process an undisarable slit appears between the manufactured head and the sheet. According to the riveting manual, a special hold-on should be used for the rivet with a compensator. For example, in the case of the 3,55 mm brazier rivet with a compensator, the most beneficial filling of the rivet hole has been obtained for the hold-on radius of 10 mm (instead of 12 mm, as indicated in the manual).

The effect of the hole callibration (cold working – the local hardening of the hole and smothing the hole surface) on the fatigue life of the riveted joints was determined. The research was carried out for five levels of callibration. The fatigue life of specimens with callibrated holes as compared to specimens with drilled or drilled and reamed holes was from 1,68 times (for the lowest level of callibration) to 11,4 times higher (for the highest level of callibration). The radial and tangential strain distribution around the callibrated hole was determined with the Laser Grating Ekstensometry System. This technique was used during fatigue tests in order to determine the callibration influence on the local strain amplitude near the hole and near the hole filled with the rivet. For the structural specimens of the commuter aircraft, a fatigue life increase of 65% for lower load levels and of 112% for higher load levels was obtained.

A wide range of fatigue tests were carried out on the riveted lap joint specimens. The specimens represented the longitudinal joints on the aircraft pressurized fuselage. Fatigue properties of riveted joints were compared. The comparison concerned two sheet materials (D16AT and 2024-T3), two types of anti-corrosion layers (alclad and alclad+anodised) and

three rivet materials (PA24, PA25 and 2117). The following design factors were considered in the fatigue tests: rivet pitch and row spacing as well as sheet thickness. The expedience of non-standard geometry of the riveted lap joint (staggered thickness joint-with stepped thickness) was examined. The effect of various squeezing forces was investigated for many of these configurations. Residual stresses around the rivet are proportional to the squeezing force value. The experimental investigation of the radial expansion of the rivet hole provided further information about the effect of squeezing force. The numerical calculation indicated that radial residual stresses are very sensitive to the removing of the rivet material (stresses decreased to 30% after removing the rivet), while tangential residual stresses remained at 80% of the previous state after removing the rivet. Radial displacements (diameter) of the hole were increasing while the rivet head was being removed and decreasing after the whole rivet shank was removed.

The fatigue tests have proved that the staggered thickness lap joints have better fatigue properties than standard joints. It should be emphasized that this is the first experimental confirmation of this interesting concept, which allows improving fatigue life without a weight penalty. The analyses with the Schijve model have proved that the main reason for this improvement is the reduction of the secondary bending in the outer rivet row, caused by the appropriate reduction of the sheet thickness.

An extensive program of measurements and analyses of load transfer in the lap joint was carried out in view of prospective fatigue life estimation. The program covered measurements of the lateral rivet forces in the overlap area and measurements of the rivet flexibility in relation to various squeezing forces. The results obtained enabled the verification of the currently used analytical solution of load transfer.

The fractographic analysis of the riveted lap joint has proved that the squeezing force affects the joint damage mechanism (due to the stress concentration at the hole or fretting phenomenon). The squeezing force influence should be thus taken into account in the fatigue life predictions. At the same time, the squeezing force influence on the load distribution in the joint has been proved. Therefore, the currently used analytical procedure of calculating the lateral forces in the overlap area could give incorrect results.

The new optical methods of the rivet deformations measurements were developed. They could be very useful for verification of the numerical calculations.

The theoretical analyses, confirmed with the strain gauge measurements, have indicated the presence of high secondary bending. Simple analytical methods based on the beam theory and described in the literature as a tool for estimating secondary bending in the riveting joints with the force eccentricity, the Schijve model in particular, have proved a convenient instrument for evaluation of the bending parameter, (defined as nominal bending stress in the critical rivet row divided by applied load). The validation of the Schijve model was carried out with the strain gauge measurements of bending stresses in the lap joint. The beam models' ability to adequately estimate the influence of the geometrical configuration and the load level on the secondary bending in the joints with the eccentricity was confirmed.

The FEM calculations of the lap joint and the single strap butt joint were performed. For the simple joint models, the sheets were modeled with shell elements, which lay in the sheet middle layer (secondary bending, which is the inherent feature of such joints, was taken into account). Several rivets models were tested. For the analysis of the joint with many rivets, the model consisting of shell elements as well as the GAP contact elements and rigid MPC elements was developed. This model allows taking into account secondary bending as well as contact interactions between the sheets and the rivet shank with a relatively small number of nodes and contact elements. At the first stage of the analysis, temperature was defined for rivet elements in order to introduce residual stresses. At the second stage of the analysis, the joint was tensioned by applied force or displacements. The lap joint with two rivets (two

rows) was analysed with the solid model. Geometrical and material nonlinearity was taken into account. At the first two stages, the sequential riveting process of two rivets was simulated. At the third stage, the joint was tensioned. Important strain changes on the sheet surface near the rivet were observed during tension. This phenomenon was recorded during the fatigue tests by the micro strain gauges placed in the specimen axis near the rivet manufactured head. Due to the problems with the calculation convergence, the results for high load level were not obtained.

The analysis of voids nucleated in the aluminium alloy during tension was carried out based on the SEM fractographic observations. The change in the material structure in the area of high tension was recorded. Cracks occur near the inclusions during tension of the sheet. Cracks appear at the boundary of the inclusions. In numerical simulations of structural elements, the materials are described in macroscopic terms e.g. the elasto-plastic material model which takes into account destruction of the material as a result of void growth, proposed by Gurson. This model enables a more realistic simulation of the sheet necking and observation of the slit growth during tension as well as a very exact determination of the sheet breaking moment based on the reaction value.

Comparative calculations of the stress intensity factor (SIF) for the corner crack growing from the hole – cylindrical and with the countersunk – in rectangle plates were performed using different methods. The Newman and Raju equations and FRANC3D (the boundary element method) software as well as the MSC MARC (the finite element method) software with the *Virtual Crack Closure Technique (VCCT)* were employed. Afterwards, the SIF calculation for a crack growing from one of the holes in the lap-joint specimen made of D16 alloy was performed. The fatigue tests of this specimen with crack growth measurement were carried out at the Krakow University Of Science And Technology (AGH), a member of the IMPERJA consortium. SIF Calculations for a few crack sizes were performed with the FEM and VCCT methods. The SIF for the complex load was determined as the superposition of the individual SIFs for each load component i.e. tension, bending and pin loading calculated in separate calculations. Moreover, crack growth predictions with the NASGRO equation implemented in the AFGROW software were carried out.

The possibility of fatigue life predictions with the estimated fatigue curves (in terms of strain and determined based on tensile tests) was investigated. This method was found unsuitable for 2024-T3 and D16CzATW aluminum alloy. Based on the selected loading sequence compiled with the FALSTAFF, seven methods of fatigue life estimation were verified. For the stress approach using the Wöhler diagram, the satisfactory correlation with the experiment results was obtained for the Kwofie's model. For the strain approach using the Morrow plot, the best results were obtained for the SWT parameter modified by Bergmann.

Application part of the project.

The variable amplitude (VA) fatigue tests were carried out for two types of specimens of the riveted joints in the wing and fuselage of the Commuter class aircraft .

The FEM analysis of the joint in the wing was performed at three different complexity levels, namely considering the part of the wing (three bulkheads at each side of the rib at the investigated joint, I level local model – the shell model of the joint corresponding to the specimen subjected to the fatigue tests, and II level local model – the solid model of the single rivet.

The cumulative fatigue damage calculations of the structural specimens were performed according to the method recommended by the USA Federal Aviation Administration in

AC23-13A. The fatigue curves of riveted joint were derived from the literature and developed based on the fatigue tests performed under the IMPERJA project. The results of the FEM analyses of these specimens were used for the fatigue calculations with the MSC FAIGUE software. The high scatter and poor correlation with the experimental results were observed. In the calculations, the presence of the residual stresses after the riveting process was neglected. The residual stresses were taken into account in the fatigue calculations with the PragTic software (developed by J.Papuga, Evector company). The calculations were performed with the uniaxial (Smith-Watson-Topper, Landgraf) and multiaxial (Socie) methods. The obtained results were very conservative, especially for uniaxial methods (higher for the SWT than for the Landgraf methods; the methods differ in the way of the mean stress correction). The assumed material properties heavily influence the calculation results. The nodes of the numerical model with the lowest fatigue life were not always coincident with the points where the cracks nucleated in the experimental test.

Many practical results, which could be useful for the aerospace industry, were obtained. These concern appropriate selection of the rivet geometry, size and material as well as the riveting process parameters. Especially valuable is demonstrating the dependency between the squeezing force and the fatigue life of the joints. Higher squeezing force is connected with higher radial expansion of the rivet hole, which causes generation of the residual compressive stresses around the rivet – which is beneficial from the fatigue point of view. The observation that the fatigue performance of the joint is determined by the squeezing stress rather than the relative size of the driven head, as it is commonly accepted in the industry, is of particular importance. The squeezing force effect should be taken into account in the fatigue life predictions since it influences the joint damage mechanism (due to the stress concentration at the hole or fretting).

Riveted staggered lap joints have better fatigue properties than standard joints. The fatigue tests have proved that fatigue life of the riveted joints is somewhat lower for the alclad and anodised sheets than for the alclad sheets. This observation agrees with the literature.

Based on the database generated under the project it has been demonstrated that for the lap joints of various geometrical configurations but the same sheet material, rivet type and squeezing stress, a good consolidation of the fatigue test results in the common scatter band is obtained when the fatigue lives are presented in terms of the combined tensile and bending stress amplitude.

The results of the research carried out under the project were published in one PhD thesis, six monographs (two in English) and two monograph chapters, forty-three articles (sixteen in English), forty-one conference papers (fourteen in English, presented at international conferences) and nineteen internal reports (four in English).

1. Li, G., Shi, G., Bellinger N.C.: *Studies of Residual Stress in Single-Row Countersunk Riveted Lap Joints*, Journal of Aircraft, Vol. 43, No. 3, 2006
2. Muller R. G. P., An experimental and numerical investigation on the fatigue behaviour of fuselage riveted lap joints, PhD thesis, Delft University of Technology, 1995.
3. Müller R. P.G., Hart-Smith L.J.: *Making fuselage riveting lap splices with 200-year crack-free fatigue life*. ICAF 97' „Fatigue in new and ageing aircraft”. Proceedings of the I9-th Symposium of the International Committee of Aeronautical Fatigue1997, Edinburgh, EMAS Publishing, 499-522.